

NOVEL DONOR-ACCEPTOR TYPE GREEN POLYMER BEARING  
PYRROLE AS THE DONOR UNIT WITH EXCELLENT SWITCHING TIMES  
AND VERY LOW BAND GAP AND ITS MULTICHROMIC COPOLYMERS

A THESIS SUBMITTED TO  
THE GRADUATE SCHOOL OF NATURAL AND APPLIED SCIENCES  
OF  
MIDDLE EAST TECHNICAL UNIVERSITY

BY

SELİN ÇELEBİ

IN PARTIAL FULFILLMENT OF THE REQUIREMENTS  
FOR  
THE DEGREE OF MASTER OF SCIENCE  
IN  
CHEMISTRY

SEPTEMBER 2009

Approval of thesis:

**NOVEL DONOR-ACCEPTOR TYPE GREEN POLYMER BEARING  
PYRROLE AS THE DONOR UNIT WITH EXCELLENT SWITCHING  
TIMES AND VERY LOW BAND GAP AND ITS MULTICHROMIC  
COPOLYMERS**

submitted by **SELİN ÇELEBİ** in partial fulfillment of the requirements for the  
degree of **Master of Science in Chemistry Department, Middle East Technical  
University** by,

Prof. Dr. Canan Özgen \_\_\_\_\_  
Dean, Graduate School of **Natural and Applied Sciences**

Prof. Dr. Ahmet M. Önal \_\_\_\_\_  
Head of Department, **Chemistry**

Prof. Dr. Levent Toppare \_\_\_\_\_  
Supervisor, **Chemistry Dept., METU**

**Examining Committee Members:**

Prof. Dr. Savaş Küçükyavuz \_\_\_\_\_  
Chemistry Dept., METU

Prof. Dr. Levent Toppare \_\_\_\_\_  
Chemistry Dept., METU

Prof. Dr. Duygu Kısakürek \_\_\_\_\_  
Chemistry Dept., METU

Prof. Dr. Jale Hacaloğlu \_\_\_\_\_  
Chemistry Dept., METU

Asst. Prof. Dr. Metin Ak \_\_\_\_\_  
Chemistry Dept., Pamukkale University

**Date:** \_\_\_\_\_

**I hereby declare that all information in this document has been obtained and presented in accordance with academic rules and ethical conduct. I also declare that, as required by these rules and conduct, I have fully cited and referenced all material and results that are not original to this work.**

Name, Last Name : Selin ÇELEBİ

Signature :

## ABSTRACT

### NOVEL DONOR-ACCEPTOR TYPE GREEN POLYMER BEARING PYRROLE AS THE DONOR UNIT WITH EXCELLENT SWITCHING TIMES AND VERY LOW BAND GAP AND ITS MULTICHROMIC COPOLYMERS

Çelebi, Selin

M.Sc., Department of Chemistry

Supervisor : Prof. Dr. Levent Toppare

September 2009, 87 pages

A new neutral state green polymer, poly (2,3-bis(4-tert-butylphenyl)-5,8-di(1H-pyrrol-2-yl) quinoxaline) (PTBPPQ) was synthesized and its copolymer with bis(3,4-ethylenedioxythiophene) (BiEDOT) and 4,7-bis(2,3-dihydrothieno[3,4-b][1,4]dioxin-5-yl)-2-dodecyl-2H-benzo [1,2,3] triazole (BEBT) were produced. Finally polymers' potential use as an electrochromic material was investigated. Electrochromic properties of the polymers were investigated by several methods including spectroelectrochemistry, kinetic and colorimetry studies. Key properties of conjugated polymers such as band gap, maximum absorption wavelength, the intergap states that appear upon doping and evolution of polaron and bipolaron bands were investigated via spectroelectrochemistry experiments. Switching times and optical contrasts of the homopolymer and the copolymer were evaluated via kinetic studies. Copolymer of TBPPQ with BiEDOT and BEBT were electrochemically synthesized and characterized. Resulting copolymer films have

distinct electrochromic properties and revealed multichromism through the entire visible region. Although BiEDOT and BEBT have different oxidation potentials, the resulting copolymers have very similar redox behaviors. In a monomer free solution, both copolymers show four colors from purple, gray, light green to transmissive blue with the variation of the applied potential. Copolymerization with BiEDOT and BEBT not only decreases the band gap,  $E_g$ , but also enhances the electrochromic and optical properties. Hence, electrochemical copolymerization is considered to be a powerful tool to improve the electrochromic properties of quinoxaline derivatives. It should be noted that PTBPPQ is one of the few examples of neutral state green polymeric materials with superior switching properties. Hence, PTBPPQ can be used as a green polymeric material for display technologies.

Keywords: Electrochromism, Donor-Acceptor Type Polymers, Green Polymers, Fast Switching Times, Conducting Polymers, Electrochemical polymerization, Copolymerization

## ÖZ

### MÜKEMMEL DÖNÜŞÜM ZAMANINA VE ÇOK KÜÇÜK BANT ARALIĞINA SAHİP, DONÖR GRUP OLARAK PİROL İÇEREN YENİ POLİMER VE ÇOK RENKLİ KOPOLİMERLERİ

Çelebi, Selin

Yüksek Lisans, Kimya Bölümü

Tez Yöneticisi: Prof. Dr. Levent Toppare

Eylül 2009, 87 sayfa

Nötral halinde yeşil olan poli (2,3-bis(4-tert-butylphenyl)-5,8-di(1H-pyrrol-2-yl) quinoxaline) (PTBPPQ) sentezlenmiş ve bis(3,4-ethylenedioxythiophene) (BiEDOT) ve 4,7-bis(2,3-dihydrothieno[3,4-b][1,4]dioxin-5-yl)-2-dodecyl-2H-benzo [1,2,3] triazole (BEBT)' le kopolimerizasyonu gerçekleştirilmiştir. Daha sonra bu polimerlerin potansiyel elektrokromik malzeme olarak kullanımı incelenmiştir. Sentezlenen iletken polimerlerin elektrokromik özellikleri; spektroeletrokimya, kinetik ve renk çalışmaları gibi yöntemlerle gözlemlenmiştir. Bant aralığı, maksimum soğurulan dalga boyu, katkılıandığında oluşan ara haller ve polaron ve bipolaron bantlarının oluşumu gibi iletken polimerlerin kilit özellikleri spektroeletrokimya deneyleriyle incelenmiştir. Homopolimerin ve kopolimerlerin dönüşüm zamanları ve optik kontrastlarını hesaplamak için kinetik çalışmaları yapıldı. Donör-akseptör yeşil polimerden beklendiği gibi,

homopolimer biri 408 diğeri 745 nm de olmak üzere farklı iki soğurma bandı göstermektedir. Ayrıca, homopolimer mükemmel dönüşüm zamanına (0.1 sn, 0.3 sn, 0.6 sn) ve tatmin edici optik kontrasta sahiptir. TBPPQ ile BiEDOT ve BEBT 'in kopolimeri elektrokimyasal olarak sentezlendi ve karakterizasyonu yapıldı. Sentezlenen kopolimerler farklı elektrokromik özellikler ve multikromik özellik göstermektedirler. BiEDOT ve BEBT farklı yükseltgenme potansiyellerine sahip olmalarına rağmen , sentezlenen kopolimerler birbirlerine benzer yükseltgenme-indirgenme özellikleri göstermektedirler. Monomer içermeyen çözeltide iki kopolimerde uygulanan farklı potansiyellerde mor, gri, açık yeşil ve şeffaf mavi olmak üzere dört farklı renk göstermektedirler. BiEDOT ve BEBT ile yapılan kopolimerizasyon hem bant aralığının azalmasını, hemde elektrokromik ve optik özelliklerin daha iyi olmasını sağlamıştır. Bu durum, elektrokimyasal kopolimerizasyonun kinokzalin türevlerinin elektrokromik özelliklerinin güçlendirilmesi için çok yararlı bir yöntem olduğunu göstermiştir. Unutulmamalıdır ki PTBPPQ iyileştirilmiş dönüşüm zamanlı, nötral halinde yeşil nadir polimerlerdendir. Bu yüzden, PTBPPQ görüntü teknolojisinde kullanılabilecek yeşil polimerik malzemedir.

Anahtar Kelimeler: Elektrokromizm, Donör-Akseptör Tipi Polimerler, Yeşil Polimerler, Hızlı Dönüşüm Zamanları, İletken Polimerler, Elektrokimyasal polimerizasyon, Kopolimerizasyon.

**TO MY FAMILY AND GRANDMOM**



## ACKNOWLEDGMENTS

I would like to express my deepest gratitude to my thesis supervisor Prof. Dr. Levent Toppare for his endless guidance and patience throughout my study and also his trust in me. It's my pleasure to work with such an intelligent and talented person.

I also gratefully thank every single friend for being there for me and their great support. Special thanks to Derya Baran and Arzu Güven.

I would like to thank all my lab mates for their valuable helps and enjoyable friendship. Special thanks to Abidin Balan.

I am proud of being a member of Middle East Technical University and I believe I am very lucky for having a chance to study in such a self sufficient university. I want to thank all members of METU.

Finally, I am grateful to my father, mother, brothers, sisters, Çetin Kocaoğlu, Nesrin Çelebi and of course my grandmom for always supporting me. It is great to feel you by my side.

## TABLE OF CONTENTS

ABSTRACT .....	iv
ÖZ .....	vi
ACKNOWLEDGMENTS.....	ix
TABLE OF CONTENTS .....	x
LIST OF TABLES .....	xiii
LIST OF FIGURES.....	xiv
CHAPTERS	
1. INTRODUCTION.....	1
1.1    Conducting Polymers.....	1
1.1.1    Brief History.....	1
1.1.2    Band Theory.....	3
1.2    Conduction in Conducting Polymers .....	5
1.2.1    Charge Carriers .....	5
1.2.2    Doping.....	7
1.3    Polymerization Methods .....	13
1.3.1    Chemical Polymerization .....	13
1.3.2    Electrochemical Polymerization.....	14
1.4    Chromism.....	15
1.4.1    Electrochromism .....	16
1.4.2    Factors Affecting the Band Gap and the Color of Conducting Polymer .....	18
1.5    Donor-Acceptor Theory and Low Band Gap Systems.....	21
1.6    Conducting Copolymer .....	25
1.7    Neutral State Green Polymeric Materials .....	27
1.7.1    Donor-Acceptor Methods Towards Green Polymeric Materials .....	28
1.8    Aim of this Work .....	30
2. EXPERIMENTAL .....	31

2.1	Materials .....	31
2.2	Equipments .....	31
2.2.1	Nuclear Magnetic Resonance (NMR) Spectrometer .....	31
2.2.2	Mass Spectrometer .....	32
2.2.3	Cyclic Voltammetry (CV) .....	32
2.2.4	UV-Vis-NIR Spectrophotometer .....	32
2.2.5	Colorimeter.....	32
2.3	Procedures.....	32
2.3.1	Monomer Synthesis .....	32
2.3.1.1	2,3-Bis(4-tert-butylphenyl)-5,8-dibromoquinoxaline.....	32
2.3.1.2	tert-Butyl Pyrrole-1-carboxylate .....	33
2.3.1.3	<i>N</i> -(tert-Butoxycarbonyl)-2-(trimethylstannyl)pyrrole .....	34
2.3.1.4	5,8-Bis[N-(tert-butoxycarbonyl)-2-pyrrolyl]2,3-bis(4-tert-butylphenyl) quinoxaline .....	35
2.3.1.5	5,8-Bis[2-pyrrolyl]2,3-bis(4-tert-butylphenyl)quinoxaline (TBPPQ) .....	36
2.3.2	Polymer Synthesis .....	37
2.3.2.1	Homopolymerization of TBPPQ .....	37
2.3.2.2	Copolymerization of TBPPQ with BiEDOT .....	38
2.3.2.3	Copolymerization of TBPPQ with BEBT .....	38
2.4	Characterization of Polymer Films .....	39
2.4.1	Cyclic Voltammetry .....	39
2.4.2	Conductivity Measurements .....	42
2.4.3	Spectroelectrochemistry .....	44
2.4.4	Switching Properties.....	44
2.4.5	Colorimetry .....	45
3.	RESULTS AND DISCUSSION .....	47
3.1	Characterization of the D-A-D Molecules .....	47
3.1.1	2,3-bis(4-tert-butylphenyl)-5,8-dibromoquinoxaline (TBPB) .....	47
3.1.2	5,8-Bis[N-(tert-butoxycarbonyl)-2-pyrrolyl]2,3-bis(4-tert-butylphenyl) quinoxaline 49	
3.1.3	5,8-Bis [2-pyrrolyl] 2,3-bis(4-tert-butylphenyl)quinoxaline (TBPPQ) .....	50
3.2	Electrochemical and Electrochromic Properties of Donor-Acceptor-Donor Type Polymers .....	52

3.2.1	Electrochemical and Electrochromic Properties of Poly(2,3-bis(4-tert-butylphenyl)-5,8-di(1H-pyrrol-2-yl) quinoxaline) (PTBPPQ).....	52
3.2.1.1	Electrochemistry of 2,3-bis(4-tert-butylphenyl)-5,8-di(1H-pyrrol-2-yl) quinoxaline (TBPPQ) .....	52
3.2.1.2	Spectroelectrochemistry of Poly(2,3-bis(4-tert-butylphenyl)-5,8-di(1H-pyrrol-2-yl) quinoxaline) (PTBPPQ).....	54
3.2.1.3	Electrochromic switching of Poly(2,3-bis(4-tert-butylphenyl)-5,8-di(1H-pyrrol-2-yl) quinoxaline) (PTBPPQ).....	56
3.2.2	Electrochemical and Electrochromic Properties of Poly(2,3-bis(4-tert-butylphenyl)-5,8-di(1H-pyrrol-2-yl) quinoxaline-co-bi-etylenedioxy thiophene) P(TBPPQ-co-BiEDOT) 59	
3.2.2.1	Electrochemistry of Poly(2,3-bis(4-tert-butylphenyl)-5,8-di(1H-pyrrol-2-yl) quinoxaline-co-bi-etylenedioxy thiophene) P(TBPPQ-co-BiEDOT) .....	59
3.2.2.2	Spectroelectrochemistry of Poly(2,3-bis(4-tert-butylphenyl)-5,8-di(1H-pyrrol-2-yl) quinoxaline-co-bi-etylenedioxy thiophene) P(TBPPQ-co-BiEDOT) .....	61
3.2.2.3	Electrochromic switching of Poly(2,3-bis(4-tert-butylphenyl)-5,8-di(1H-pyrrol-2-yl) quinoxaline-co-bi-etylenedioxy thiophene) P(TBPPQ-co-BiEDOT) .....	64
3.2.3	Electrochemical and Electrochromic Properties of Poly(2,3-bis(4-tert-butylphenyl)-5,8-di(1H-pyrrol-2-yl)quinoxaline-co-4,7-bis(2,3-dihydrothieno [3,4-b][1,4]dioxin-5-yl)-2-dodecyl-2H-benzo[1,2,3] triazole) P(TBPPQ-co-BEBT) .....	67
3.2.3.1	Electrochemistry of Poly(2,3-bis(4-tert-butylphenyl)-5,8-di(1H-pyrrol-2-yl) quinoxaline-co-4,7-bis(2,3-dihydrothieno[3,4-b][1,4]dioxin-5-yl)-2-dodecyl-2H-benzo [1,2,3] triazole) P(TBPPQ-co-BEBT) .....	67
3.2.3.2	Spectroelectrochemistry of Poly(2,3-bis(4-tert-butylphenyl)-5,8-di(1H-pyrrol-2-yl) quinoxaline-co-4,7-bis(2,3-dihydrothieno[3,4-b][1,4]dioxin-5-yl)-2-dodecyl-2H-benzo [1,2,3] triazole) P(TBPPQ-co-BEBT).....	69
3.2.3.3	Electrochromic switching of Poly(2,3-bis(4-tert-butylphenyl)-5,8-di(1H-pyrrol-2-yl) quinoxaline-co-4,7-bis(2,3-dihydrothieno[3,4-b][1,4]dioxin-5-yl)-2-dodecyl-2H-benzo [1,2,3] triazole) P(TBPPQ-co-BEBT).....	72
4.	CONCLUSION .....	76
	REFERENCES.....	78

## LIST OF TABLES

### TABLES

Table 3.1 Optical contrasts and related switching times of TBPPQ .....	59
Table 3.2 Electrochromic Properties of TBPPQ-co-BiEDOT .....	64
Table 3.3 Optical Contrasts and Related Switching Times of P(TBPPQ-co-BiEDOT) .....	66
Table 3.4 Comparison of PTBPPQ, P(TBPPQ-co-BEBT) and PBEBT in terms of $E_g$ and $\lambda_{max}$ values .....	71
Table 3.5 Electrochromic Properties of P(TBPPQ-co-BEBT) .....	72
Table 3.6 Comparison of PTBPPQ, P(TBPPQ-co-BiEDOT) and P(TBPPQ-co-BEBT) in terms of transmittances and switching times.....	75

## LIST OF FIGURES

### FIGURES

Figure 1. 1 Common conducting polymers.....	2
Figure 1. 2 Band structures of insulator, semiconductor, conductor .....	4
Figure 1. 3 Generation of bands in conjugated polymer systems .....	5
Figure 1. 4 Formation of polaron and bipolaron in polyacetylene.....	6
Figure 1. 5 Reversible doping-dedoping process of polythiophene.....	7
Figure 1. 6 Charge carriers in PPy and its corresponding energy gaps in the mid gap.....	8
Figure 1. 7 a) p-doping and b) n-doping of conducting polymer.....	10
Figure 1. 8 Conductivities of some conducting polymers with selected dopants .	12
Figure 1. 9 Chemical synthetic routes for polyheterocycles .....	14
Figure 1. 10 Electrochemical synthetic routes to polythiophene .....	14
Figure 1. 11 Structural representation of bipolaron formation in polypyrrole and its corresponding energy bands in the mid gap.....	17
Figure 1. 12 Planarity effects on band gap and the electrical and optical properties of conjugated polymers .....	20
Figure 1. 13 Planarity effects on band gap and the electrical and optical properties of conjugated polymers .....	22

Figure 1. 14 Overview of methods for the modification of band gap.....	24
Figure 1. 15 The Donor-Acceptor approach, alternating donor and acceptor moieties results in a polymer that has the combined optical properties of the parent donor or acceptor monomers.....	25
Figure 1. 16 Poly(3-methylthiophene) (P3MT), poly(2,3-di(thien-2-yl)thieno[3,4- b]pyrazine) (PDDTP) and poly(3,4-ethylenedioxythiophene) (PEDOT) were the red, green and blue colored polymers respectively. ....	28
Figure 1. 17 Combined spectroelectrochemistry of P3MT, PDDTP and PEDOT in the a) neutral state b) oxidized state.....	29
Figure 2. 1 Synthetic route of acceptor unit.....	33
Figure 2. 2 Synthetic route for the stannylation and the protection reaction of pyrrole .....	35
Figure 2. 3 Schematic representation of coupling reaction.....	36
Figure 2. 4 Schematic representation of deprotection reaction of TBPPQ.....	37
Figure 2. 5 Schematic representation of copolymerization of TBPPQ and BiEDOT. ....	38
Figure 2. 6 Schematic representation of copolymerization of TBPPQ and BEBT. .....	39
Figure 2. 7 a) Typical Potential–Time excitation signal in CV b) CV of a representative type of electroactive monomer. ....	41
Figure 2. 8 A simple four-probe measurement setup.....	43
Figure 2. 9 Square wave voltammetry .....	45

Figure 2. 10 CIELAB color space.....	46
Figure 3. $^1\text{H}$ -NMR spectrum of TBPB.....	48
Figure 3. $^{13}\text{C}$ -NMR spectrum of TBPB .....	48
Figure 3. $^3\text{H}$ -NMR spectrum of TBPEQ with t-boc.....	49
Figure 3. $^{13}\text{C}$ -NMR spectrum of TBPPQ with t-boc.....	50
Figure 3. 5 $^1\text{H}$ -NMR spectrum of TBPPQ .....	51
Figure 3. 6 $^{13}\text{C}$ -NMR spectrum of TBPPQ.....	51
Figure 3. 7 Repeated potential scan electropolymerization of TBPPQ ( $10^{-2}$ M) at 100 mV/s in 0.1 M TBAPC in DCM/ACN (5/95, v/v) on ITO electrode vs Ag wire after 40 cycles .....	53
Figure 3. 8 Scan rate dependence of PTBPPQ film on Pt vs Ag wire in 0.1 M TBAPC/ACN (a) 100, (b) 150, (c) 200, (d) 250, (e) 300 mV/s.....	54
Figure 3. 9 Spectroelectrochemistry of PTBPPQ film on ITO-coated glass slide in a monomer free, 0.1 M TBAPC/ACN electrolyte–solvent couple at applied potentials (V) vs Ag wire: (a) $-0.5$ , (b) $-0.4$ , (c) $-0.3$ , (d) $-0.2$ , (e) $-0.1$ , (f) $0.0$ , (g) $0.1$ , (h) $0.15$ , (i) $0.2$ , (j) $0.25$ , (k) $0.3$ , (l) $0.35$ , (m) $0.4$ , (n) $0.45$ , (o) $0.5$ , (p) $0.6$ , (q) $0.7$ , (r) $0.8$ , (s) $0.9$ , (t) $1.0$ , and (u) $1.1$ .....	55
Figure 3. 10 Electrochromic switching, percent transmittance change monitored at 1480 nm for PTBPPQ in 0.1 M TBAPC/ACN .....	57
Figure 3. 11 Electrochromic switching, percent transmittance change monitored at 408 nm for PTBPPQ in 0.1 M TBAPC/ACN .....	58
Figure 3. 12 Electrochromic switching, percent transmittance change monitored at 745 nm for PTBPPQ in 0.1 M TBAPC/ACN .....	58



Figure 3. 13 Cyclic voltammetry of a) P(TBPPQ-co-BiEDOT) b) TBPPQ c) BiEDOT in 0.1M TBAPC/ACN/DCM at scan rate of 100 mV/s .....	61
Figure 3. 14 Spectroelectrochemistry of P(TBPPQ-co-BiEDOT) as a function of applied potential between -0.5 and 0.9 V in 0.1 M TBAPC/ACN: (a) -0.5, (b) -0.8, (c) -0.6, (d) -0.4, (e) -0.2, (f) 0.0, (g) +0.4, (h) 0.9 V vs Ag wire.....	63
Figure 3. 15 Electrochromic switching, optical absorbance change monitored at 510 nm and 1320 nm for P(TBPPQ-co-BiEDOT) in 0.1 M TBAPC/ACN..	66
Figure 3. 16 Cyclic voltammetry of a) P(TBPPQ-co-BEBT) b) TBPPQ c) BEBT in 0.1M TBAPC/ACN/DCM at scan rate of 100 mV/s .....	68
Figure 3. 17 Linear relationship between scan rate and peak current of P(TBPPQ-co-BiEDOT) and P(TBPPQ-co-BEBT) films in monomer free, 0.1M TBAPC/ACN solution .....	69
Figure 3. 18 Spectroelectrochemistry of P(TBPPQ-co-BEBT) as a function of applied potential between -0.5 and 0.9 V in 0.1 M TBAPC/ACN : (a) -0.5, (b) -0.4, (c) 0.0, (d) 0.1, (e) 0.2, (f) 0.3, (g) 0.35, (h) 0.4, (i) 0.45, (j) 0.5, (k) 0.55 (l) 0.6, (m) 0.65, (n) 0.7, (o) 0.75, (p) 0.8, (q) 0.9 vs Ag wire .....	70
Figure 3. 19 Electrochromic switching, optical absorbance change monitored at 540 nm and 1320 nm for P(TBPPQ-co-BEBT) in 0.1 M TBAPC/ACN.....	74

## CHAPTER 1

### INTRODUCTION

#### 1.1 Conducting Polymers

##### 1.1.1 Brief History

Conducting polymers (CPs) are the new generation of polymers containing  $\pi$ -electron backbone responsible for their conducting properties.

The history of conducting polymers dates back to 60's [1]. The first conducting polymer was the inorganic polymer sulfur nitride, (SN)<sub>x</sub>, which was discovered in 1973, showed properties very close to those of a metal. The room temperature conductivity of (SN)<sub>x</sub> was of the order of  $10^3$  S/cm [2] (copper has a conductivity of  $1 \times 10^6$  S/cm, and polyethylene,  $10^{-14}$  S/cm). The first electrochemical synthesis of a conducting polymer (polyaniline) was reported by Letheby in 1862 [3].

The modern era of conducting polymers began at the end of the 1970's when Heeger and MacDiarmid discovered that polyacetylene, ((CH)<sub>x</sub>), synthesized by Shirakawa's method, could undergo a 11 order of magnitude increase of conductivity upon charge-transfer oxidative doping with iodine [4,5]. Alan Heeger, Alan MacDiarmid, and Hideki Shirakawa were awarded with The Nobel Prize in Chemistry "for the discovery and development of electrically conducting polymers" in 2000. Despite high conductivity of polyacetylene film in doped form, the material is unstable against oxygen or humidity. In order to enhance the

processability of PA by means of increasing its stability and solubility, PA derivatives were synthesized and tested. Unfortunately, the electrical conductivities of the PA derivatives were much lower than that of PA. In 1980's polyheterocycles (Figure 1.1), which were more air stable than polyacetylene, were first developed and helpful in designing new monomers due to their lower polymer oxidation potential. New classes of conducting polymers include polythiophene (PTh), polyfuran, polypyrrole (PPy), poly(p-phenylene) (PPP), poly(pphenylene vinylene) (PPV), poly(paraphenylene sulphide) (PPS) and polyaniline (PANI). However, due to the instability of these conducting polymers in the doped state, they could not be used as highly conducting metals for electrical transport and batteries but used as electrochromic rearview mirrors [6], polymer light-emitting diodes [7], organic solar cells [8], gas sensors [9], thin-film transistors [10] and electrochromic devices [11].

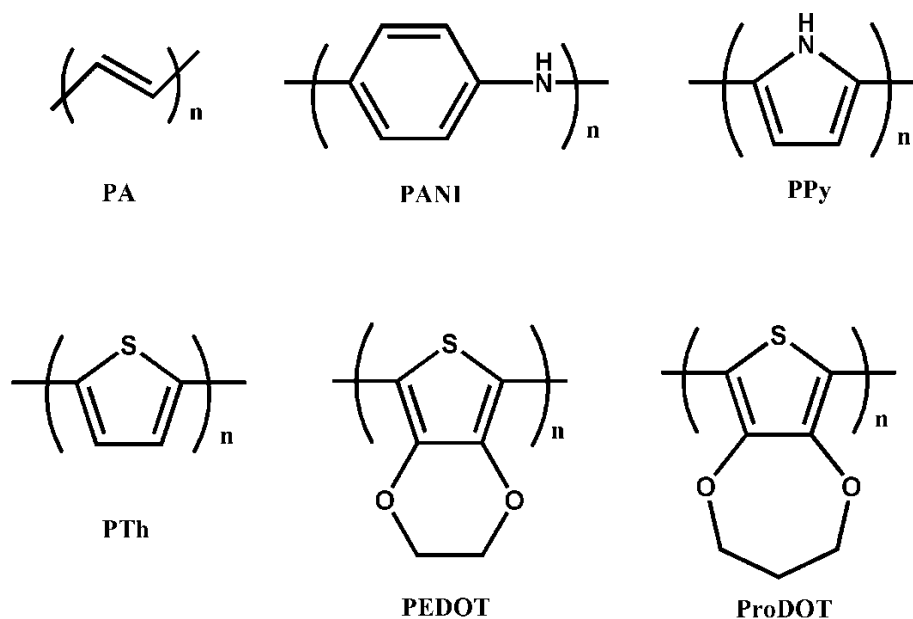


**Figure 1. 1 Common conducting polymers**

### 1.1.2 Band Theory

According to their conductivity properties at room temperature, materials can be classified into three categories; conductors, semiconductors and insulators. It is believed that electronically conducting polymers have a spatially delocalized band-like electronic structure and they are extensively conjugated molecules. In polymeric materials conduction may be explained using the band theory. Band theory says that extended delocalized energy bands are formed by the overlapping of atomic orbitals and accordingly the conductivity depends on the relative population of each band and on the energy difference between bands. The electrical properties of direct-gap inorganic semiconductors are figured out by their electronic structures, and the electrons move within discrete energy states which are referred as bands.

Similarly, the bonding and antibonding  $\pi$  orbitals of the  $sp^2$  hybridized  $\pi$ - electron materials such as polyenes generate energy bands that are fully occupied  $\pi$  and empty  $\pi^*$  band [12]. Neutral conjugated polymers are thought to be semiconductors. The highest occupied electronic levels that constitute the valence band (VB) and the lowest unoccupied levels that constitute the conduction band (CB) are the two discrete energy bands that conjugated polymers generate. The difference between these two bands or bandgap ( $E_g$ ), between the VB and CB, determines the intrinsic electrical properties of the material [13]. Band gap refers to onset energy of the  $\pi$ - $\pi^*$  transition in neutral conjugated polymers. The band gap of a polymer can be estimated from the onset of absorption of the  $\pi$  to  $\pi^*$  transition in the UV-VIS spectrum. Another method to calculate the band gap is to measure the oxidation and reduction potentials of the polymer. The energy difference between oxidation and reduction potentials gives the band gap [14]. Extra energy is required for the movement of electrons from the VB to the CB. Moreover, the bands should be partially filled in order to have electrical

conductance; because neither empty bands nor full ones can carry electricity. Metals have high conductivities due to presence of partially filled energy bands (Figure 1.2).

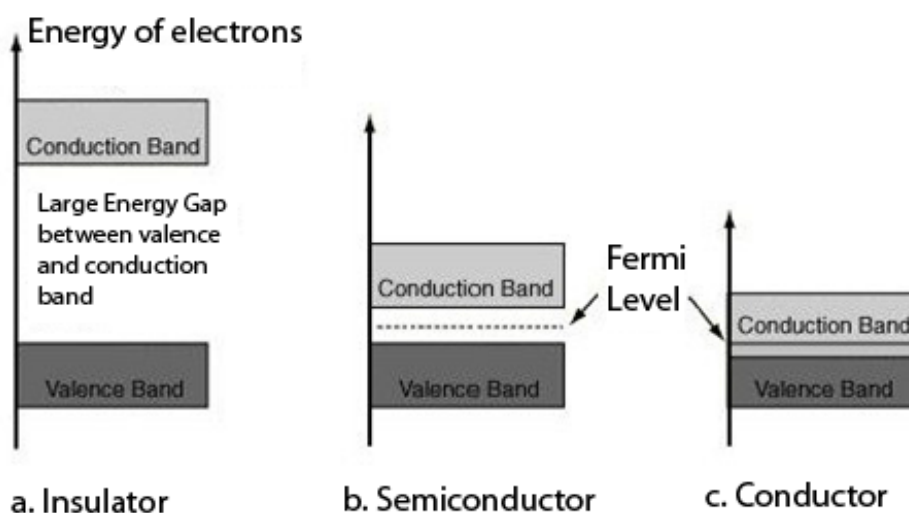


**Figure 1. 2 Band structures of insulator, semiconductor, conductor**

However, the energy bands of insulators and semiconductors, are either completely full or completely empty. In conjugated polymers, narrower band gaps, and doping can change their band structures by either taking electrons from the valence band (p- doping) or adding electrons to the conduction band (n- doping) [15]. The interaction of the  $\pi$ -orbitals of the repeating units throughout the chain constitute the band structure of a conjugated polymer [16] (Figure 1.3).

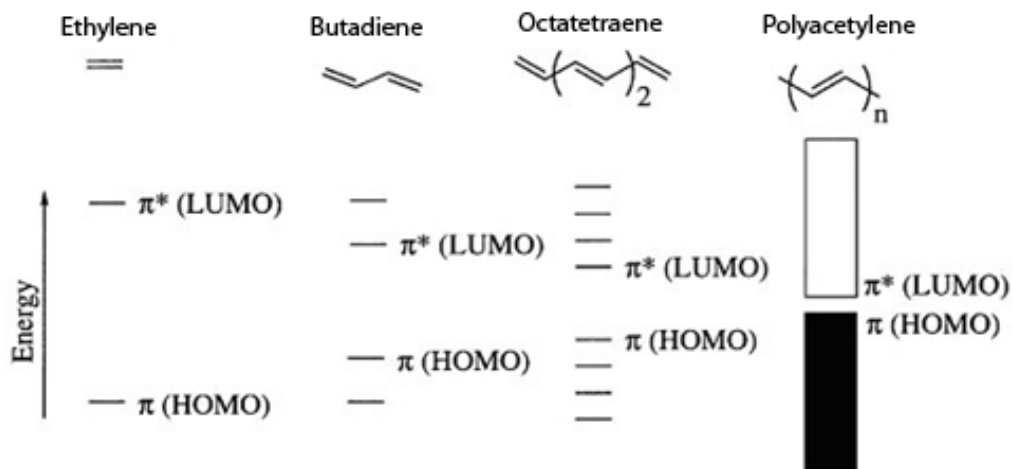


**Figure 1. 3 Generation of bands in conjugated polymer systems**

As the number of repeating units increase, the electronic levels display a one-dimensional band of allowed energies, instead of discrete energies. Interactions between adjacent  $\pi$ -electrons of conjugated polymers lead to two and three-dimensional band structure [17].

## **1.2 Conduction in Conducting Polymers**

### **1.2.1 Charge Carriers**

A good understanding of electronic conduction in polymers is the result of extensive research in the field. Electronic conduction is achieved by the transport of charge carriers through a medium (metal, polymer, etc.) under the influence of electric field. These charge carriers are electrons, holes, polarons, solitons, etc.

Soliton is a charge defect, which can be classified into three categories: neutral soliton, positive soliton and negative soliton. Neutral solitons have spin but no charge; however, charged solitons have no spin. To obtain positively charged soliton the insertion of acceptor band (p-type doping) or removal of an electron from localized state of a neutral soliton by oxidation is needed. On the other hand, negatively charged soliton is produced when an electron, donor band is inserted by reduction (Figure 1.4).

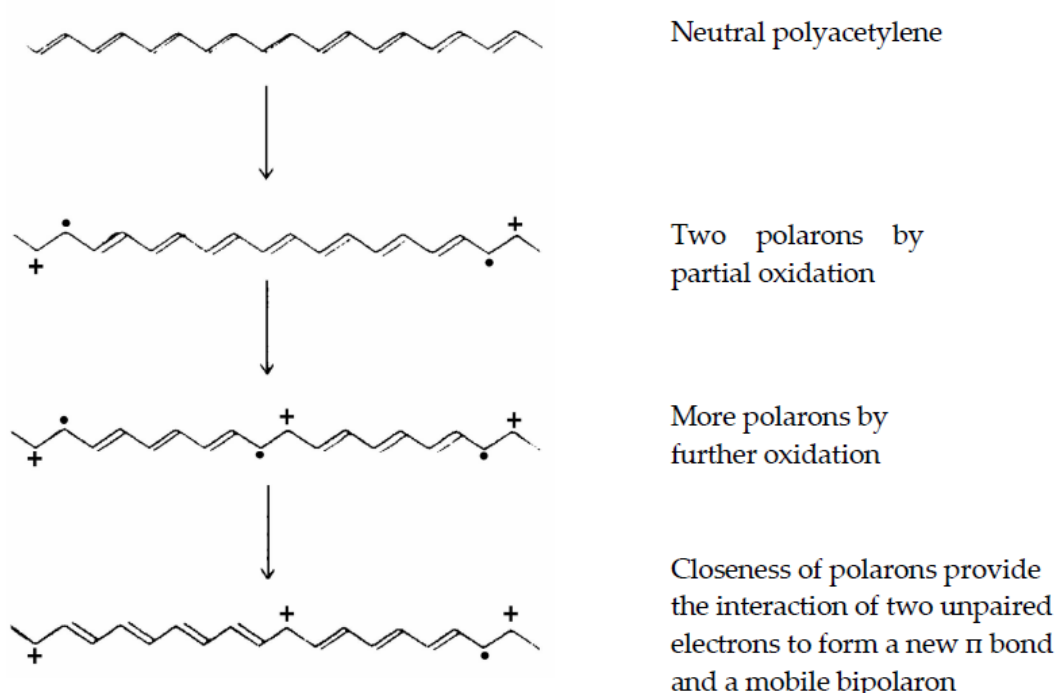


**Figure 1. 4 Formation of polaron and bipolaron in polyacetylene**

Polaron is a radical cation (radical anion), which has a spin of  $\frac{1}{2}$ , is the combination of a neutral and a charged soliton on the same polymer chain. It

partially delocalized over some polymer segment as a result of cleavage of a double bond in the polymer backbone by oxidation (reduction). Further oxidation causes more and more polarons to form and ultimately the unpaired electron of the polaron is removed, or two polarons can combine to form dication or bipolarons [18, 19]. Two charges associated with the localized polymer segment is a dication or a bipolaron. Therefore, low oxidation produces polarons, and bipolarons are formed at higher oxidation potentials.

### 1.2.2 Doping

It is possible to control the electrical conductivity of a polymer over the range from insulating to highly conducting (metallic) state. This process which enhances the conductivity of a polymer by incorporating a certain “impurity” is defined as doping. The process involves the partial addition (reduction) or removal (oxidation) of electrons to or from the  $\pi$ -system of the polymer backbone [20-22].

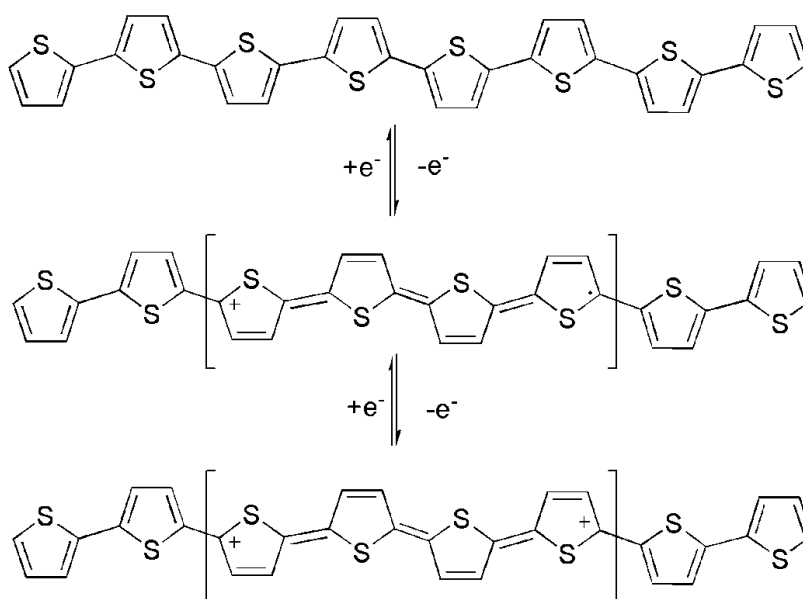


**Figure 1. 5 Reversible doping-dedoping process of polythiophene**



To obtain a conductivity anywhere between the non-doped (insulation or semiconducting) and the fully doped (highly conducting) form of the polymer, the doping level can be adjusted (Figure 1.6) [23].

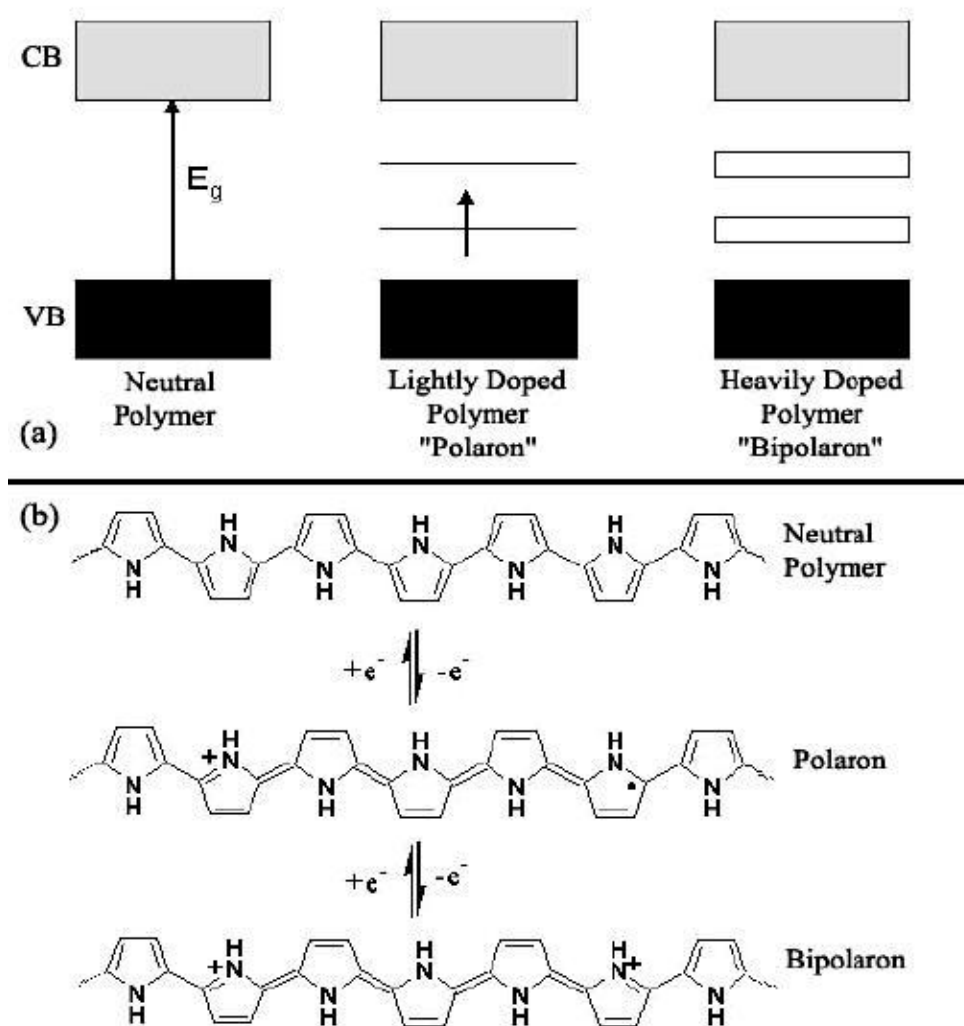


**Figure 1. 6 Charge carriers in PPy and its corresponding energy gaps in the mid gap**

Doping is a reversible process with little or no degradation of the polymer backbone. Both doping and undoping processes, involving dopant counterions which stabilize the doped state, may be carried out chemically and electrochemically [24]. Photo-doping and charge-injection doping, which introduce no dopant ions are also known [25].

Chemical doping can be performed either by reaction with gaseous species, such as  $\text{AsF}_3$ ,  $\text{PF}_3$ ,  $\text{I}_2$ , or in solution by reaction with aqueous  $\text{FeCl}_3$ . Generally, sodium naphthalide ( $\text{Na}^+\text{Npt}^-$ ) is used to perform n-type doping of a polymer in tetrahydrofuran solution.

While attempting to obtain intermediate doping levels, inhomogeneous doping makes this process difficult to control, although it is an efficient and straightforward process. To solve this problem, electrochemical doping was invented [26].

Electrochemical doping is most useful and easy way to control doping process. It is easy to oxidize or reduce the polymer electrochemically by adjusting appropriate potential in an electrochemical cell [27]. In reduction process, the electrode gives electrons to the conjugated polymer. For oxidation process, the electrode accepts electrons from the conjugated polymer. The charge on the polymer chain is then neutralized by the counter ion from the electrolyte solution [28]. Figure 1.7 represents a schematic illustration of the band diagrams for the p-doping (a) and n-doping (b) of a conducting polymer [29].

Whether electrons are extracted (p-doping) or inserted (n-doping) the process is determined by the relative positions of the Fermi level of the substrate ( $E_F, m$ ) with respect to either the valence band ( $E_{VB}, p$ ) or the conduction band ( $E_{CB}, p$ ) of the polymer the relative. In p-doping process; a flow of electrons form the

polymer to the substrate will occur if the Fermi level of the substrate is below the valence band of the polymer, (Figure 1.7 (a)). On the other hand, in n-doping process; electrons flow into the film if the Fermi level of the substrate is above the conduction band of the conducting polymer (Figure 1.7 (b)).

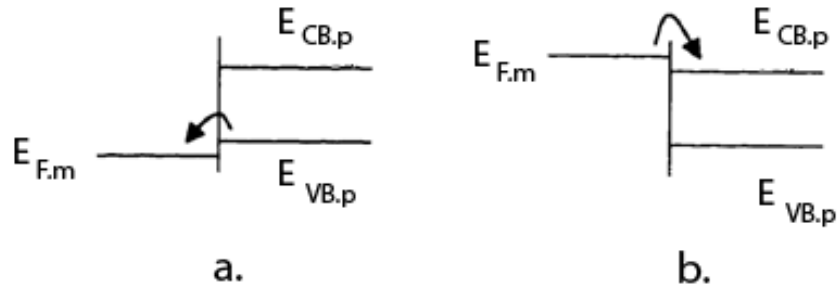
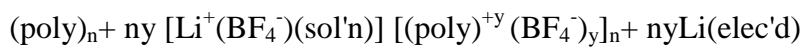


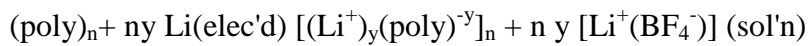
**Figure 1. 7 a) p-doping and b) n-doping of conducting polymer**

Electrochemical doping is illustrated by the following examples:

For p-type:

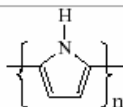
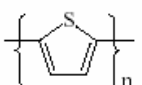
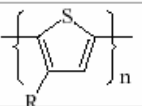
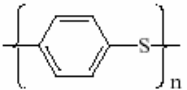
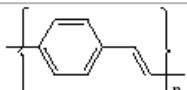
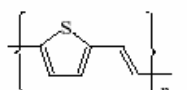
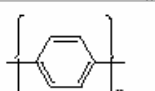
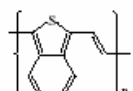
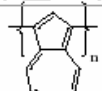
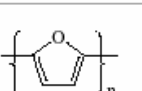
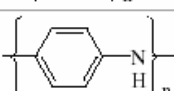


For n-type:



where sol'n is solution and elec'd is electrode.

Doping agents or dopants can be either strong reducing or oxidizing agents. They may be neutral molecules and compounds or inorganic salts, which can easily form ions. The nature of dopants, play an important role in the stability of conducting polymers [30]. In Figure 1.8 conductivities of some conducting polymers with selected dopants are displayed.

Polymer	Structure	Doping materials	$\Omega^{-1}\text{cm}^{-1}$
Polyacetylene	$(\text{CH})_n$	$\text{I}_2$ , $\text{Br}_2$ , Li, Na, $\text{AsF}_5$	10000
Polypyrrole		$\text{BF}_4^-$ , $\text{ClO}_4^-$	500-7500
Polythiophene		$\text{BF}_4^-$ , $\text{ClO}_4^-$	1000
Poly(3-alkylthiophene)		$\text{BF}_4^-$ , $\text{ClO}_4^-$	1000-10000
Polyphenylene sulfide		$\text{AsF}_5$	500
Polyphenylenevinylene		$\text{AsF}_5$	10000
Polythienylenevinylene		$\text{AsF}_5$	2700
Polyphenylene		$\text{AsF}_5$ , Li, Na	1000
Polyisothianaphthene		$\text{BF}_4^-$ , $\text{ClO}_4^-$	50
Polyazulene		$\text{BF}_4^-$ , $\text{ClO}_4^-$	1
Polyfuran		$\text{BF}_4^-$ , $\text{ClO}_4^-$	100
Polyaniline		HCl	200

**Figure 1. 8 Conductivities of some conducting polymers with selected dopants**

### **1.3 Polymerization Methods**

There are several numbers of methods to synthesize conducting polymers [30] which are mainly chemical polymerization, electrochemical polymerization, photochemical polymerization, metathesis polymerization, concentrated emulsion polymerization, inclusion polymerization, solid-state polymerization, plasma polymerization, pyrolysis and soluble precursor polymer preparation. Conducting polymers that are stable in both conducting and undoped states and soluble in certain solvents were synthesized in order to obtain new and novel structures, where the order of the polymer backbone as well as conductivity was increased.

#### **1.3.1 Chemical Polymerization**

In chemical polymerization which is the least expensive, most simple, and most widely used chemical synthesis of conducting polymers [31,32] stoichiometric amount of oxidizing reagent is used to produce polymer in its doped or conducting form. Heterocyclic monomers are usually polymerized with  $\text{FeCl}_3$  as the chemical oxidant [32,33] although other oxidants can also be employed (Figure 1.9) [32,34]. Reduction to the neutral state is accomplished by the addition of a strong base such as ammonium hydroxide or hydrazine.

Chemical polymerization occurs in the bulk of the solution, and the resulting polymers precipitate as insoluble solids [35] having limiting degree of polymerization. Overoxidation and decomposition may also occur in these polymerizations if strong oxidizing agents are used [36].

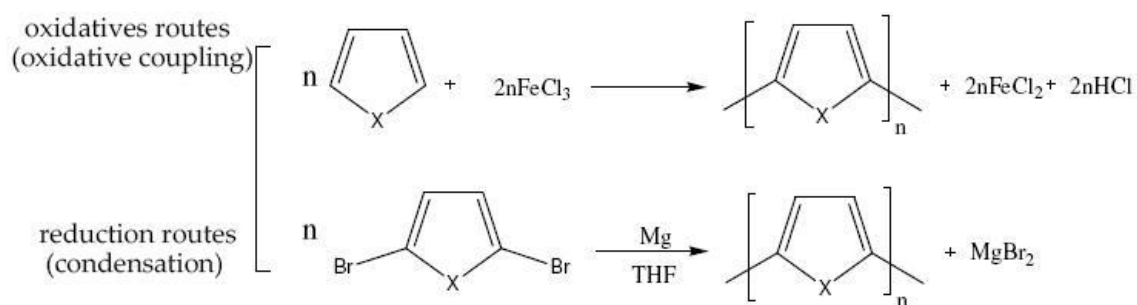


**Figure 1. 9 Chemical synthetic routes for polyheterocycles**

### 1.3.2 Electrochemical Polymerization

Electropolymerization is achieved by the electro-oxidation of the heterocycle in an inert organic solvent containing supporting electrolyte. Electrochemical syntheses of poly(heterocycles) have been carried out by an anodic or a cathodic route (Figure 1.10).

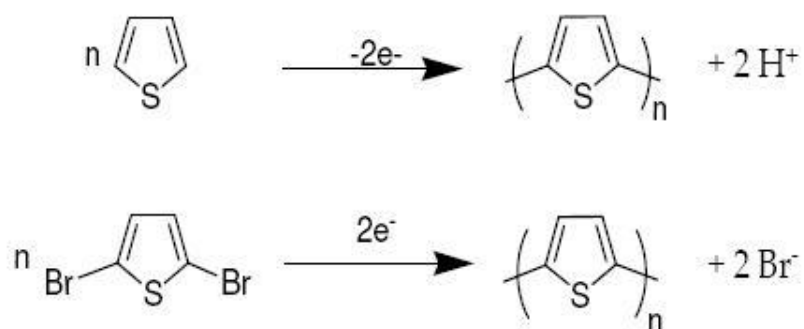


**Figure 1. 10 Electrochemical synthetic routes to polythiophene**

Electrochemical synthesis is a simple, selective and reproducible method where the type of solvent, electrolyte system, choice and concentration of monomer and electrodes strongly affect the properties of the final conducting polymer [37].

Compared with other chemical and electrochemical methods, the advantages of oxidative electropolymerization are [38,39]:

- (i) A highly electrochemically active and conductive polymer film can be easily produced on an electrode, which can be directly used as an electrode in a battery or a sensor.
- (ii) Film thickness, morphology and conductivity can be easily controlled by the applied potential, polymerization time, and the electrochemical potential scan rate.
- (iii) They provide an in situ way to investigate the polymerization process and the properties of the resulting conducting polymer by electrochemical or spectroscopic techniques.

#### **1.4 Chromism**

Chromic behavior is another characteristic of CPs which is a change in color brought about by the corresponding environmental changes. Types of chromism reported are thermochromism, solvatochromism, piezochromism, ionochromism and electrochromism for CPs. These different chromic behaviors originate from conformational modification and the energy change in  $\pi$ - $\pi^*$  transition band gap induced by the corresponding environmental changes. These environmental changes are temperature, solvent power, pressure, ion strength, and applied potential, respectively [40].



### 1.4.1 Electrochromism

Electrochromism is a color change brought about by an electrochemical redox reaction. A material can be defined as electrochromic when it reveals drastic color changes upon electrochemical oxidation or reduction.

There is a vast number of chemical species possessing electrochromic properties. Viologens [41], transition metal oxides, most famously tungsten trioxide ( $\text{WO}_3$ ) systems [42-44], prussian blue systems [45], phthalocyanines [46, 47], and conducting polymers [17] are widely utilized as electrochromic materials. Due to their advantages over inorganic compounds, conducting polymers attract more attention than inorganic materials. Some of these properties are fast switching ability, high coloration efficiency, fine tuning of the band gap through chemical structure modification and possibility of having multiple colors within the same material [48].

Electrochromism arises from the energy difference between the  $\pi$ -bonding and the  $\pi^*$ -antibonding orbitals. The optical properties of these materials can be adjusted by controlled doping (and/or dedoping).

As mentioned in Section 1.2.2, the doping process of a conducting polymer involves a structural modification of the backbone from a totally aromatic neutral form to a doped state with quinoidal partitions [49]. This change in structure introduces new electronic states in the band gap with a decrease in the intensity of the  $\pi$ -to- $\pi^*$  transition and the formation of lower energy transitions leads to the color changes. The bipolaron states overlap in bipolaron bands; the bipolaron bands may appear between valence and conduction bands as doping level is increased. Evolutions of band structure and color changes are given in Figure 1.11.

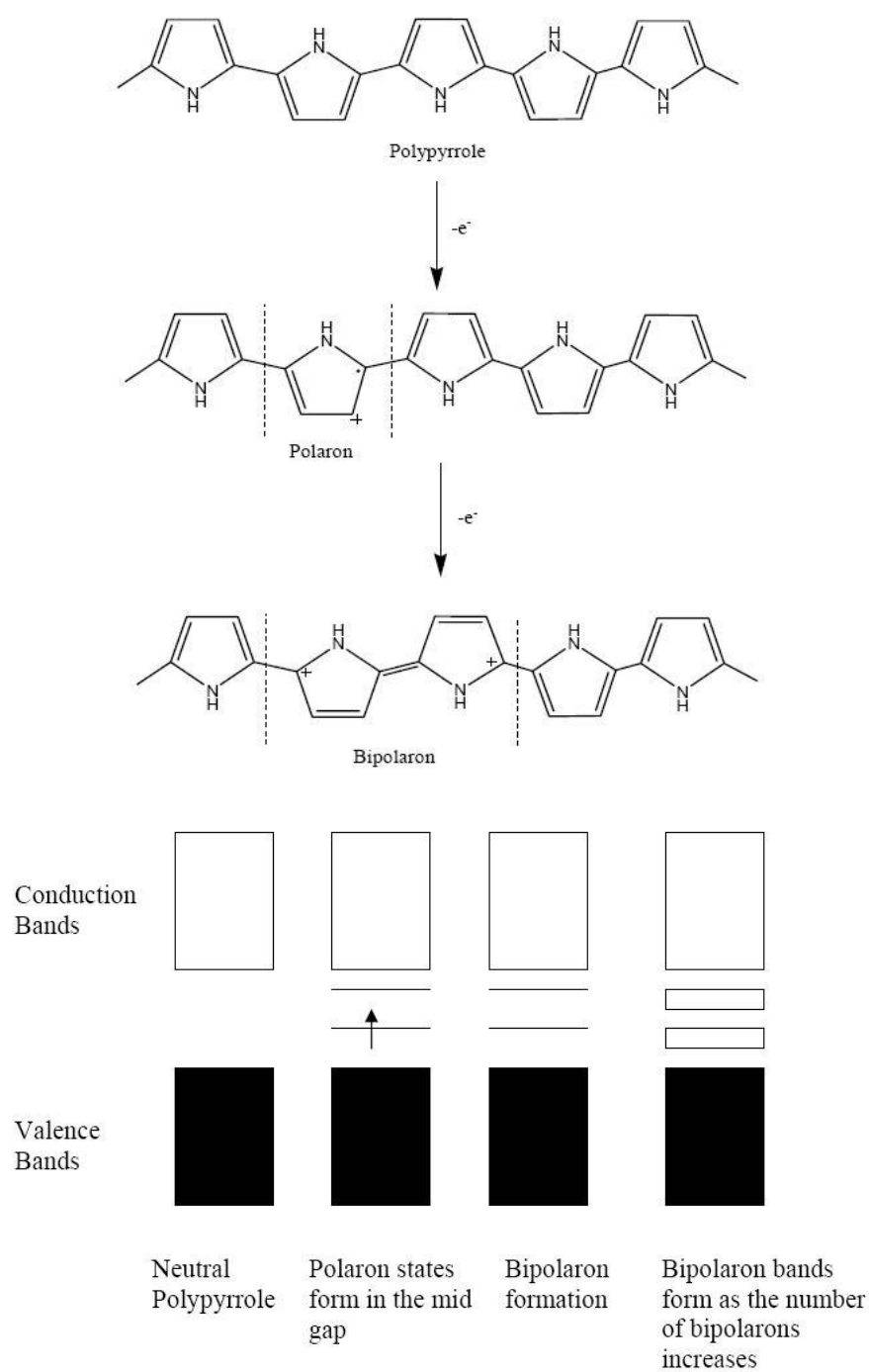


**Figure 1. 11 Structural representation of bipolaron formation in polypyrrole and its corresponding energy bands in the mid gap**

The main electronic transition occurring in neutral polymers is the  $\pi-\pi^*$  transition. In the neutral state, the color is determined by the band gap ( $E_g$ ) of the polymer. The magnitude of the energy gap of the undoped polymer determines the color contrast between doped and undoped forms of the polymer [50]. The mean conjugation length of the polymer, different polymerization routes and different experimental conditions such as current density, starting molecule concentration, electrolytic medium and temperature are some factor that affect  $E_g$ .

#### 1.4.2 Factors Affecting the Band Gap and the Color of Conducting Polymer

It becomes important to control the electronic properties especially band gap of  $\pi$ -conjugated systems since the color of polymer depends on the band gap energy. In the neutral state of the polymer, the color depends on the energy gap between the valence and conduction bands. The energy gap between bipolaron band and conduction band determines the color in oxidized state. These characteristics are all related to the conjugation of polymer, the electrochemical nature of side groups and their effects on the polymer backbone. The band gap is influenced by energy related to the bond length alternation ( $E_{BLA}$ ), the mean deviation from planarity ( $E_\theta$ ), the aromatic resonance energy ( $E_{Res}$ ), the inductive and mesomeric electronic effects of substituents ( $E_{Sub}$ ) and interchain interactions ( $E_{Int}$ ). As a result of that the band gap of a material derived from a linear  $\pi$ -conjugated system can be expressed by the sum of these five affects: [51].

$$E_g = E_{BLA} + E_{Res} + E_{Sub} + E_\theta + E_{Int}$$

Owing to the results in a competition between  $\pi$ -electron confinement within the rings and delocalization along the chain, aromaticity in poly(aromatics) hence, the band gap of conjugated polymer generally decreases with a decrease in the resonance energy per electron [52].

Bond alternation is defined as the maximum difference between the length of a C-C bond inclined relative to the chain axis and a C-C bond parallel to the chain axis [53]. One of the most efficient approaches for gap reduction is the conversion of a polyaromatic chain into a conjugated system with an enhanced quinoid character. The band gap of a polymer can be drastically decreased as the quinoid geometry of the polymer increased. The property of polyisothianaphthene is one of the most important examples of this effect. [52]. Benzene, with energy of aromatization of 1.56 eV, is more aromatic than thiophene (1.26 eV). These forces (PITN) to be more energetically stable in the quinoidal state, which provides for a lowered band gap of 1.1 eV compared to polythiophene with a band gap of 2.0 eV.

Therefore, the major contribution to the magnitude of the energy gap is from bond length alternation energy (EBLA). As a result of that, to decrease the band gap, researchers focused on structural modifications resulting in a reduced BLA [54].

The classical example of aromaticity control in conjugated polyheterocycles is polyisothianaphthene (PITN), a polythiophene with a benzene ring fused at the 3- and 4-positions along the polymer backbone [52]. Single bonds between the aromatic cycles cause interannular rotations in conjugated polymers. This twist angle varies with the overlap of the orbitals and causes the departure from coplanarity. The decline in the extent of overlap leads to an increase of  $E_g$  by a quantity of EQ. This knowledge led researchers to design and synthesize highly planar systems. The high planarity in polyacene systems achieved by excluding all the single bonds in the polymer backbone resulting in all  $\pi$  conjugated polymeric systems [55].

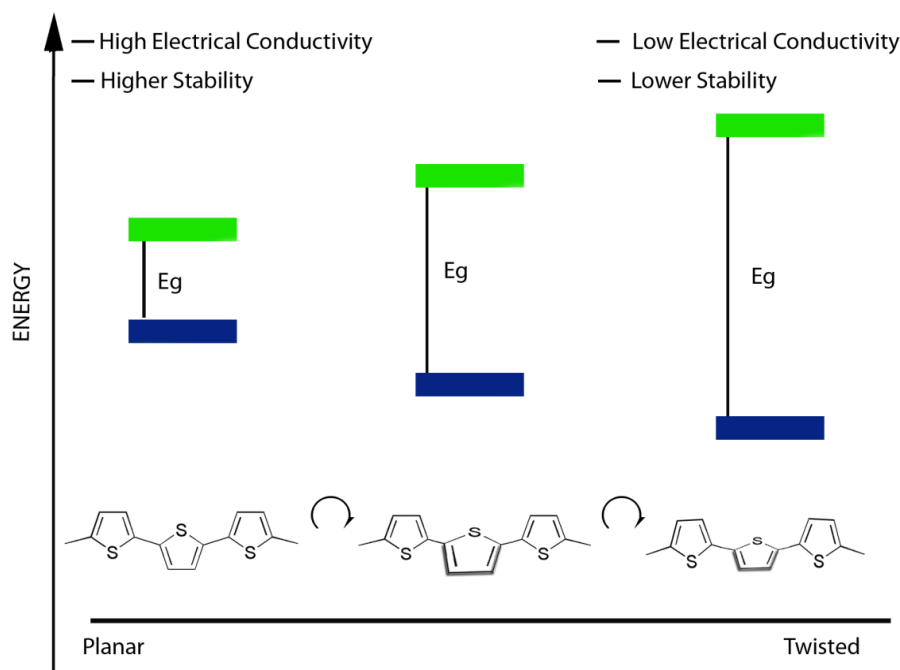


**Figure 1. 12 Planarity effects on band gap and the electrical and optical properties of conjugated polymers**

The introduction of electron-donating substituents onto a conjugated chain raises the energy of the valence band electrons (HOMO of the conjugated chain) which leads to decrease the polymer's oxidation potential and thereby decreases the band gap by  $E_{\text{Sub}}$ . Electron releasing or withdrawing substituents are also known to increase the HOMO and lower the LUMO respectively.

Additionally, the cross-linking during the polymer synthesis was found to result in non-processable and hard to characterize materials. To overcome this problem it stands as a sensible idea to perform di-substitution on thiophene ring at the 3,4 positions. However, the poly(3,4-dialkylthiophenes) are turned out to have higher oxidation potentials, higher optical band gaps and lower conductivities owing to

the steric interactions between the substituents which makes this approach unsuccessful [54]. Fusing the ring onto the heterocycle, effective pinning of the substituents back from the main chain, solved this problem as was the case of poly(3,4- ethylenedioxythiophene).

## **1.5 Donor-Acceptor Theory and Low Band Gap Systems**

$\pi$ -Conjugated polymers with donor-acceptor moieties have gained attention due to the facility of ready manipulation of the HOMO/LUMO levels (electronic structure), which leads to small band gap semiconducting polymers and enhance third-order nonlinear optical properties of the materials [56,57]. Minimizing the band gap is an important goal since small band gaps maximizes conductivity of the neutral CPs.

Polymers having band gaps greater than 2 eV are called mid- to high band gap, those having lower than 1.5 eV are considered relatively low band gap materials. There are few examples available in the literature with band gaps below 0.8 eV [53].

As discussed in detail in section 1.4.2 there have been many methodologies developed in the design and synthesis of low band gap systems. The five main approaches are;

Controlling bond-length alternation (Peierls Distortion),  
Creating highly planar systems,  
Inducing order by interchain effects,  
Resonance effects along the polymer backbone,  
Donor-Acceptor Approach.

Bond-length alternation is the difference in the length of single and double bonds along the polymer backbone. The quinoidal form has a much lower band gap than the aromatic state.

A number of researchers have utilized many different methods to achieve highly planar low band gap systems because the higher the torsional angle between adjacent rings the larger the band gap of a system (Figure 1.13).

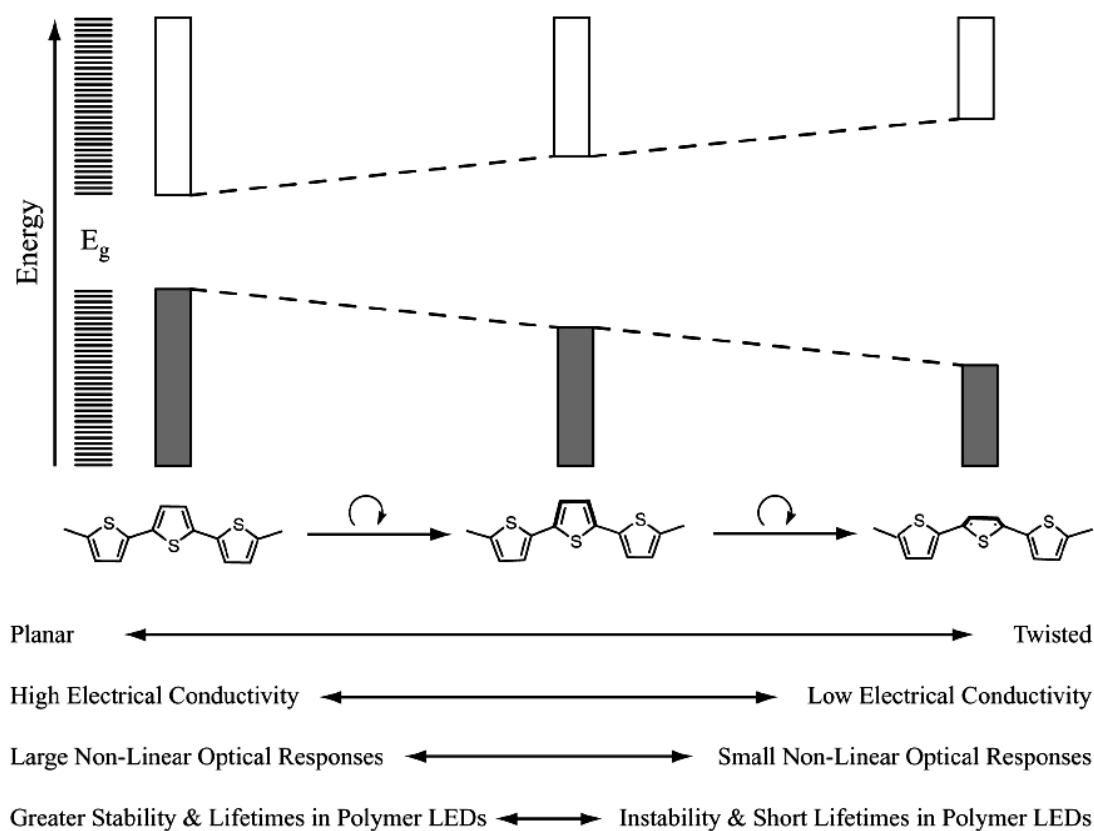


**Figure 1. 13 Planarity effects on band gap and the electrical and optical properties of conjugated polymers**

PITN is a notable example of one of the earliest low band gap polymers, since there exists a competition between aromatic and quinoid geometries in the polymer structure [51]. As it is mentioned in the section 1.4.2 PITN has lower band gap than that of PTh. Polymerization of ITN occurs through 2 and 5 positions of the thiophene ring. Since it is impossible for thiophene and benzene to be aromatic simultaneously, this arrangement induces a competition for aromaticity in the monomer repeat. Due to the high energy of aromatization benzene predicted to remain aromatic and force thiophene to adopt a pseudo-diradical electronic state at the 2 and 5 positions which makes thiophene units to be in the quinoid form and lowers the band gap of the system by decreasing bond length alternation.

Although there are many promising polymer synthesized by the approaches discussed above, during recent years synthesis of donor-acceptor type polymers was proven to be superior compared to the other methods. Donor-Acceptor approach generally divided into two different groups;

The first one is the polymers with acceptor group that directly have resonance interaction on the polymer backbone (with aromatic and quinoid forms) and the second one is the polymers with an acceptor group that inductively modify the polymer backbone. (Figure 1.14)



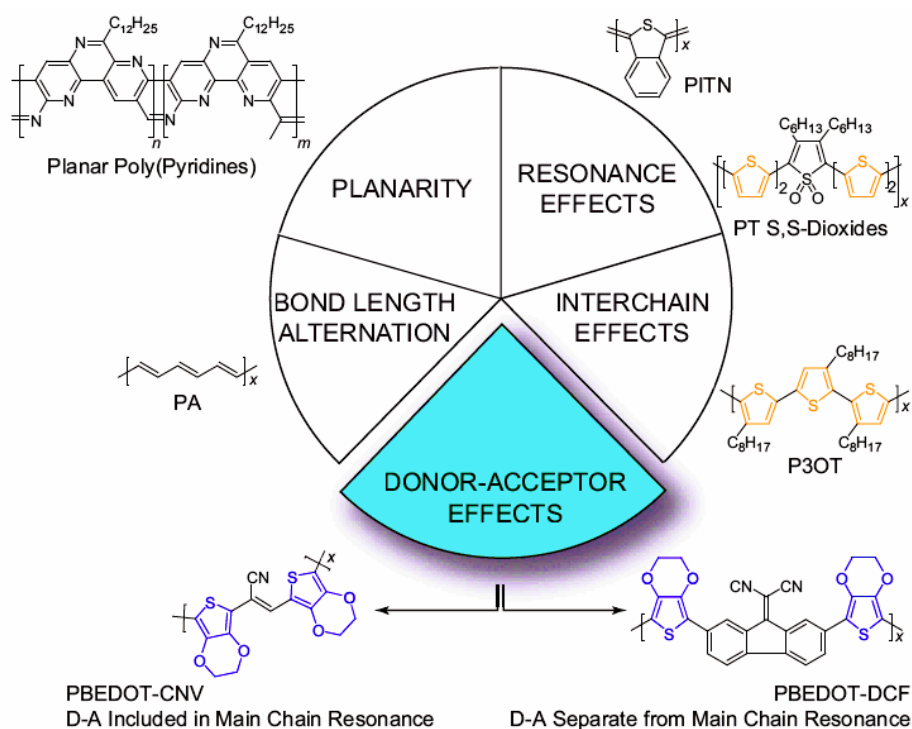


**Figure 1. 14 Overview of methods for the modification of band gap**

Due to resonances that enable a stronger double bond character between the donor and acceptor units, donor–acceptor systems lead to a narrower bandgap which in return leads to a decrease in bond length alternation. This is attributed to hybridization between the energy levels, especially the HOMO of the donor and the LUMO of the acceptor [58]. The idea is to combine having high HOMO level of the donor and low level of the LUMO of the acceptor in the same polymer to induce a lower band gap. Figure 1.15 illustrates the concept of the donor-acceptor approach (D-A) for PEDOT [59], poly(cyanoacetylene) (PCA) [60] and PBEDOT-CNV. According to D-A theory, the resulting polymer has very similar

valence band energy of the donor moiety and has a very close conduction band energy value of the acceptor moiety which makes a tremendously decrease in band gap compared to both PEDOT and PCA.

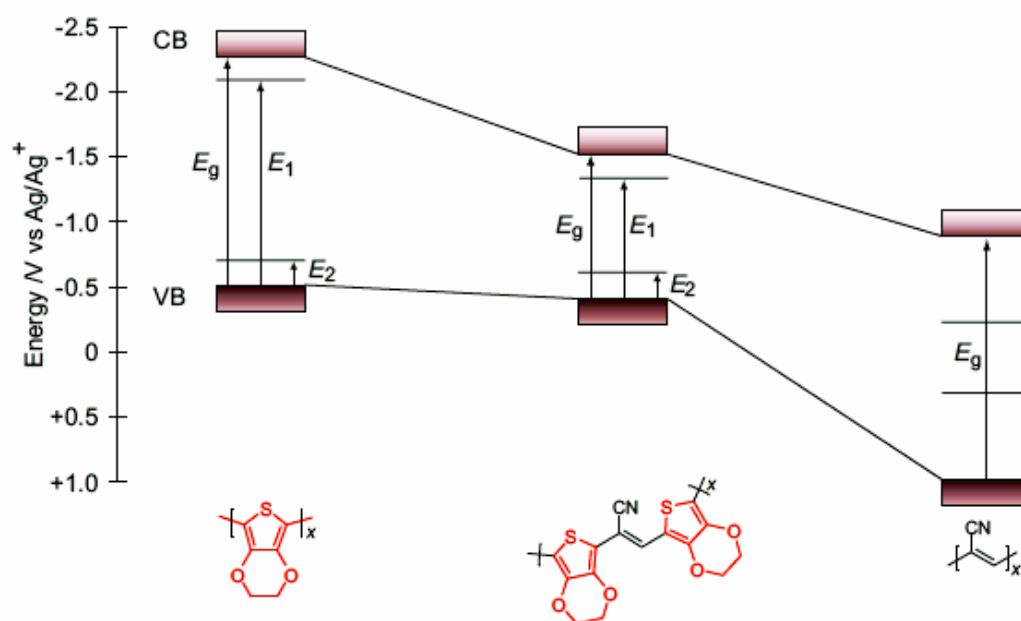


**Figure 1. 15 The Donor-Acceptor approach, alternating donor and acceptor moieties results in a polymer that has the combined optical properties of the parent donor or acceptor monomers.**

## 1.6 Conducting Copolymer

Copolymerization, a process in which two or more monomers are incorporated as integral segments of a polymer, is used to produce copolymers with properties that are different from those of corresponding homopolymers.

Due to their ease of synthesis, good environmental stability, and long term stability of electrical conductivity, conducting polymers are promising materials; however, there are several drawbacks restricting their processing and applications for practical use. The  $\pi$ -electron system along the polymer backbone leads to rigidity and crosslinking. The crosslinking in the polymer chain makes it insoluble, hard, brittle and therefore, poorly processable [61]. Copolymers generally possess physical and mechanical properties intermediate between both homopolymers. These properties generally depend on the concentration of the monomer units incorporated into the copolymer. It is very important that copolymerization leads to a homogeneous material, which its properties can be regulated by adjusting the ratio of the concentration of monomer in the feed [62].

Those materials can be prepared either chemically or electrochemically. There are three methods to be employed in electrochemical synthesis. One of which is to copolymerize the monomer with another monomer. The second method uses an electrolyte solution that contains both the monomer and the host polymer. Third one is the polymerization of the conducting component on electrode previously coated with the insulating host polymer.

Electrochemical synthesis of copolymer films from pyrrole and substituted pyrroles [63,64] pyrrole and thiophene [65], bithiophene [66] and other combination of aromatic compounds [67] have been reported in the literature. Today, the synthesis of copolymer is mainly performed with 3,4-ethylenedioxythiophene (EDOT) or bis-3,4-ethylenedioxythiophene (BiEDOT). These materials are superior to their parent polythiophene in many categories crucial to organic electrochromic materials such as rapid switching and lower oxidation potentials [68]. In this way, the resultant copolymer could indicate better electrochemical and optical properties than its homopolymers.

## 1.7 Neutral State Green Polymeric Materials

In the history of polymeric electrochromic materials, the most important breakthroughs for the commercialization of these materials, is the discovery of a neutral state green polymer. There are a number of electrochromic polymers reflecting red and blue color in their neutral states [69,70] in the literature whereas few studies have been reported related to polymers reflecting green color [71-73]. In order to have red or blue color in reduced state, the materials have to absorb at only one dominant wavelength. On the contrary, for a green color, there should exist at least two simultaneous absorption bands in the red and blue regions of the visible spectrum where these bands should be controlled with the same applied potential. These phenomena have been fulfilled with ground-breaking work of Sonmez et al in 2004 and the first neutral state green polymer was characterized [71].

It is important to state that by structural modification of a conjugated polymer system, many differently colored polymers can be achieved [74,75]. A variety of colors can be produced by using different polymers in their neutral, intermediate, p-doped and n-doped states [75]. On the other hand, by keeping color mixing theory in mind, it would be possible to cover entire visible spectrum by having materials that have three primary colored polymers in their neutral state. Theoretically, if two colors are mixed, the resulting color has to be somewhere on the line connecting the two points on the chromaticity diagram.

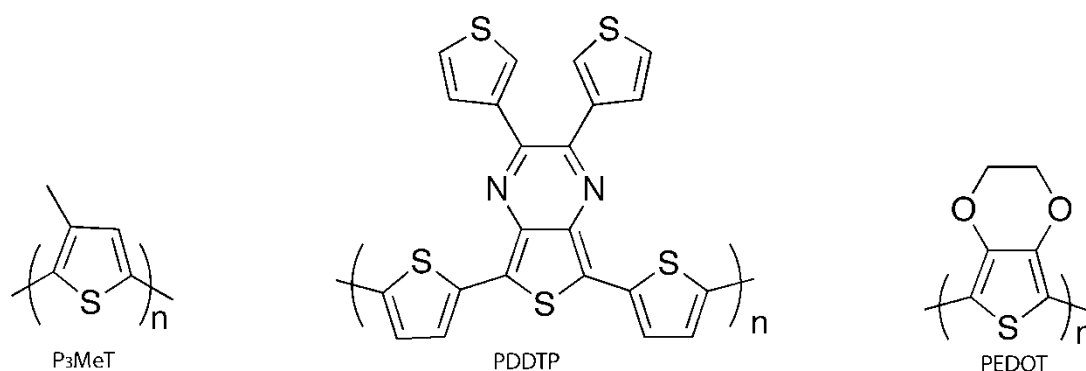


**Figure 1. 16 Poly(3-methylthiophene) (P3MT), poly(2,3-di(thien-2-yl)thieno[3,4- b]pyrazine) (PDDTP) and poly(3,4-ethylenedioxythiophene) (PEDOT) were the red, green and blue colored polymers respectively.**

The polymers P3MT, PDDTP and PEDOT have proven to have highly saturated RGB colors in their neutral state respectively. Red P3MT and blue PEDOT show only one absorption maximum whereas green PDDTP shows two. These two absorption bands are controlled together with the same applied potential. A combination of these three spectra covers the entire visible region without reflecting any light that produces a black color. Colors vanish as RGB colored polymers are oxidized, thereby producing a pale blue color for the polymers P3MT and PEDOT and a transmissive brown color for PDDTP (Figure 1.16).

### **1.7.1 Donor-Acceptor Methods Towards Green Polymeric Materials**

Since there are few conducting polymers having green color in its neutral state, it is very important to synthesize new ones. This can be only achieved utilizing donor-acceptor approach [76]. In the literature there are many examples that

donor-acceptor type polymers have two  $\pi$ - $\pi^*$  transitions [77]. Due to resonance effects that enable a stronger double bond character between the donor and acceptor units, donor-acceptor systems lead to narrower band gap [78]. The regular alternation of conjugated donor and acceptor moieties in a conjugated chain which causes broadening of valence and conduction bands leads to induce a small band gap [79]. The low band gaps as low as 0.45 eV [80] have been reported. This can also be explained by hybridization between the energy levels, especially the HOMO of the donor and the LUMO of the acceptor [58].

Therefore to provide a green color to the polymer and also to provide narrower band gap, donor-acceptor approach is crucial.

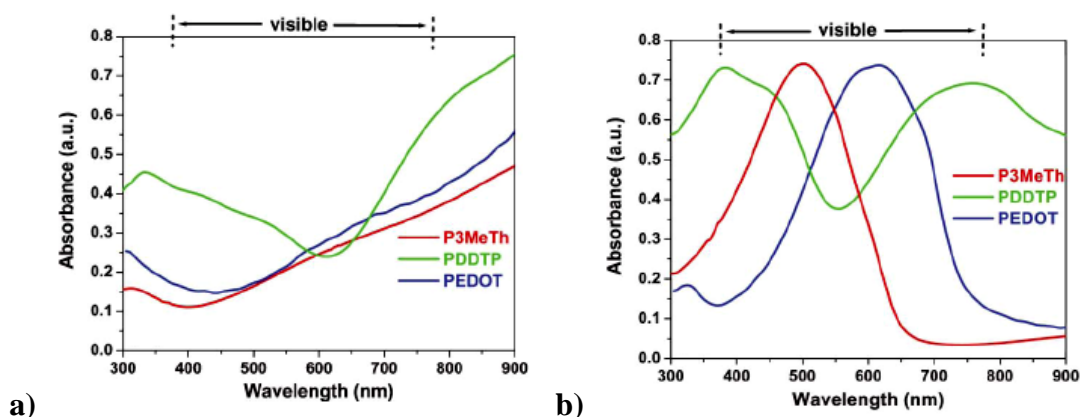


**Figure 1. 17 Combined spectroelectrochemistry of P3MT, PDDTP and PEDOT in the a) oxidized state b) neutral state**

## **1.8 Aim of this Work**

The major aim here is to synthesize donor acceptor type, neutral state green polymer. In this study pyrrole was chosen as the donor unit and as an acceptor unit 2,3-bis(4-tert-butylphenyl)quinoxaline was utilized to realize donor-acceptor type polymers. In the scope of this study other aims are; to characterize monomer, electrochemically polymerize and copolymerize it with a well known comonomer BiEDOT and with BEBT in thin film forms, investigate electrochromic and spectroelectrochemical properties of homopolymer and copolymers.

## CHAPTER 2

### EXPERIMENTAL

#### 2.1 Materials

All chemicals were purchased from Aldrich except anhydrous tetrahydrofuran (THF) which was purchased from Acros. 4,7-Dibromobenzo[1,2,5]thiadiazole [81], 3,6- dibromo-1,2-phenylenediamine [82], benzoin [83], benzyl [83], 1,2-bis(4-tert-butylphenyl)-2-hydroxyethanone [84], 1,2-bis(4-tert-butylphenyl)ethane-1,2-dione [84], 5,8-dibromo- 2,3-diphenylquinoxaline [85], tert-butyl pyrrole- 1-carboxylate [86], N-(tert-butoxycarbonyl)-2-(trimethylstannyl) pyrrole [86] were synthesized according to previously described methods. Tetrahydrofuran (THF) was distilled over Na/benzophenone prior to use.

#### 2.2 Equipments

##### 2.2.1 Nuclear Magnetic Resonance (NMR) Spectrometer

$^1\text{H}$  and  $^{13}\text{C}$  NMR spectra were recorded in  $\text{CDCl}_3$  on Bruker Spectrospin Avance DPX-400 Spectrometer and chemical shifts ( $\delta$ / ppm) were given relative to tetramethylsilane as the internal standard.



### **2.2.2 Mass Spectrometer**

Mass studies were performed using Waters Micromass Quattro Micro ac Mass Spectrometer.

### **2.2.3 Cyclic Voltammetry (CV)**

Electropolymerization was performed with a Voltalab 50 potentiostat in a three-electrode cell consisting of platinum wire or Indium Tin Oxide (ITO) coated glass as the working electrodes, platinum wire as the counter electrode, and a Ag wire as the pseudo reference electrode. Electrodeposition was performed in a 0.1 M solution of tetrabutylammonium perchlorate (TBAPC) at a scan rate of 100 mV/s for 15 cycles.

### **2.2.4 UV-Vis-NIR Spectrophotometer**

UV–Vis–NIR spectra were recorded on a Varian Cary 5000 spectrophotometer at a scan rate of 2000 nm/min.

### **2.2.5 Colorimeter**

Colorimetry measurements were performed via Minolta CS-100 Spectrophotometer.

## **2.3 Procedures**

### **2.3.1 Monomer Synthesis**

#### **2.3.1.1 2,3-Bis(4-tert-butylphenyl)-5,8-dibromoquinoxaline**

A solution of 3,6-dibromo-1,2-phenylenediamine (1.0 g, 3.8 mmol) and 1,2-bis(4-tert-butylphenyl)ethane-1,2-dione (1.223 g, 3.8 mmol) in EtOH (40 ml) was refluxed overnight by with a catalytic amount of p-toluenesulfonic acid (PTSA).

The mixture was cooled to 0 °C. The precipitate was isolated by filtration and washed several times with ethanol to afford the desired compound.

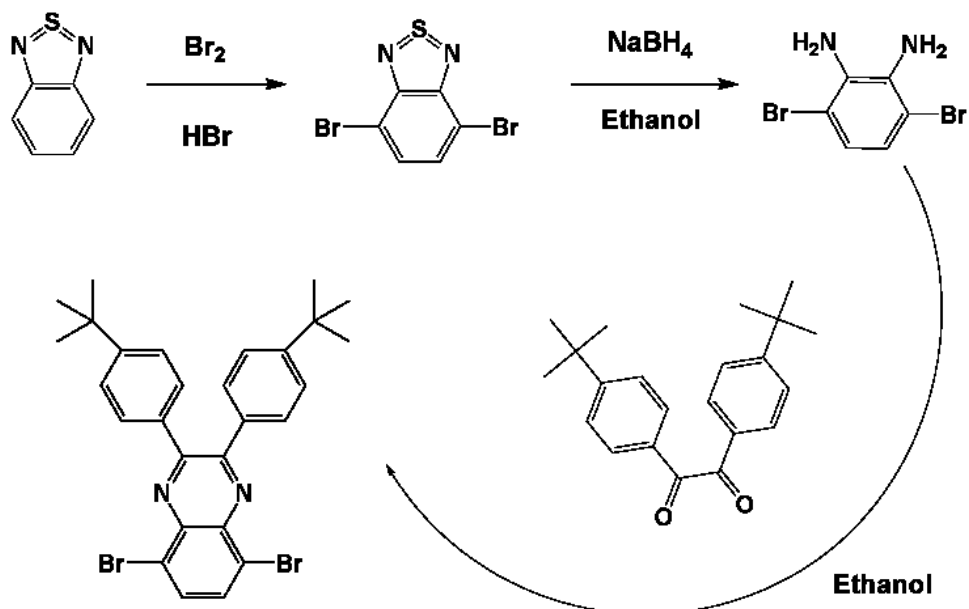


**Figure 2. 1 Synthetic route of acceptor unit**

### 2.3.1.2 *tert*-Butyl Pyrrole-1-carboxylate

Di-*tert*-butyl dicarbonate,  $(\text{Boc})_2\text{O}$ , (7.8 g, 35.7 mmol) and 4-dimethylamino)pyridine, DMAP, (0.5 g, 4.49 mmol) were added to pyrrole (2.0 g, 29.8 mmol) in acetonitrile (30 mL) under argon. After the addition was completed, the mixture was stirred at room temperature for two hours. Evaporation of the solvent and subsequent column chromatography ( $\text{Al}_2\text{O}_3$ , hexane), afforded 4.73 g (95% yield) of *tert*-butyl pyrrole-1-carboxylate as a colorless liquid.

### 2.3.1.3 *N*-(*tert*-Butoxycarbonyl)-2-(trimethylstannyl)pyrrole

A 250-mL three-necked flask equipped with magnetic stirrer, a thermometer, a dropping funnel and nitrogen gas inlet was charged with dry THF (40 mL) and 2,2,6,6-tetramethylpiperidine (2.79 g, 19.75 mmol). The mixture was cooled to –78 °C and 18 mL of a 1.6 N solution of *n*BuLi (21.5 mmol) in hexane was added slowly so that the temperature of the mixture always remained below –65 °C. The mixture was stirred for 10 min at –75 °C, then warmed to 0 °C and stirred for additional 10 min. At this point, the mixture was cooled again to –75 °C and a solution of *tert*-butyl pyrrole-1-carboxylate (3 g, 17.94 mmol) in dry THF (40 mL) was added while keeping the temperature below –65 °C. The mixture was stirred for additional 90 min while keeping the temperature below –65 °C. A solution of Bu<sub>3</sub>SnCl (7.5 mL, 23.32 mmol) in dry THF (40 mL) was added dropwise to the reaction mixture. The reaction was stirred for 40 min at –75 °C and additional 40 min at 0 °C and then for 12 h at room temperature. After removal of the THF under reduced pressure, water (50 mL) and diethyl ether (50 mL) were added to the crude and the aqueous phase was extracted with three portions of diethyl ether. The combined organic layers were dried (MgSO<sub>4</sub>) and the solvent was evaporated under reduced pressure. Column chromatography (Al<sub>2</sub>O<sub>3</sub>, hexane) of the resulting oil afforded 6.18 g (75% yield) of as a yellow liquid.

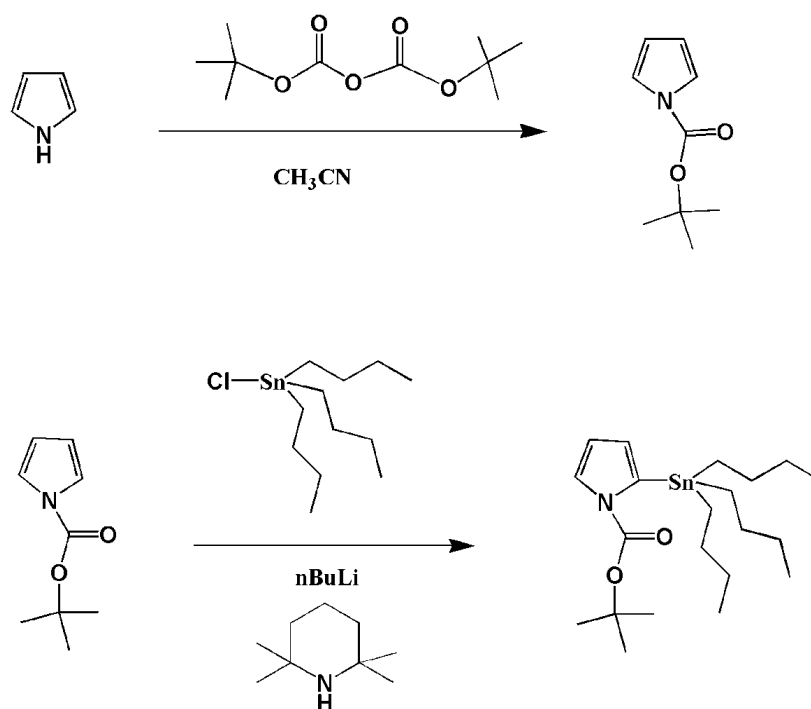


**Figure 2. 2 Synthetic route for the stannylation and the protection reaction of pyrrole**

#### **2.3.1.4 5,8-Bis[N-(tert-butoxycarbonyl)-2-pyrrolyl]2,3-bis(4-tert-butylphenyl) quinoxaline**

5,8-Dibromo-2,3-bis(4-tert-butylphenyl) quinoxaline (550 mg, 1.0 mmol), and N-(tert-butoxycarbonyl)-2-(tributylstannyl) pyrrole (2.29 g, 5.0 mmol) were dissolved in anhydrous THF (150 ml) and purged with argon for 30 min. Then, dichlorobis(triphenyl phosphine)-palladium(II) (75 mg, 0.068 mmol) was added at room temperature under argon atmosphere. The mixture was refluxed for 3 days. Solvent was evaporated under vacuum and the crude product was purified by

column chromatography on neutral alumina (eluent DCM:hexane, 2:1 v/v) to obtain 456 mg (63%) of 5,8-bis[N-(tert-butoxycarbonyl)-2-pyrrolyl] 2,3-bis(4-tert-butylphenyl) quinoxaline.

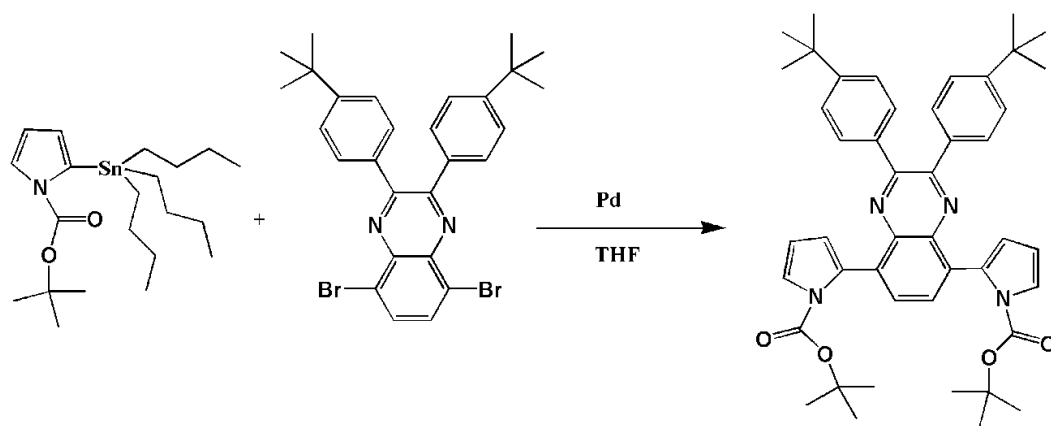


**Figure 2. 3 Schematic representation of coupling reaction**

#### 2.3.1.5 5,8-Bis[2-pyrrolyl]2,3-bis(4-tert-butylphenyl)quinoxaline (TBPPQ)

5,8-Bis [N-(tert-butoxycarbonyl)-2-pyrrolyl] 2,3-bis(4-tert-butylphenyl) quinoxaline (350 mg, 0.48 mmol) was dissolved in 60 ml methanol. 120 mg Na, (5.2 mmol) were added and the reaction mixture was heated under reflux for 24 h. The solvent was evaporated and the residue was treated with water and extracted with dichloromethane. The organic extracts were dried over  $\text{MgSO}_4$ , the solvent was evaporated and the residue chromatographed on a column with silica gel using hexane:DCM (2:1 v/v) as eluent. 180 mg (72%) TBPPQ was isolated.

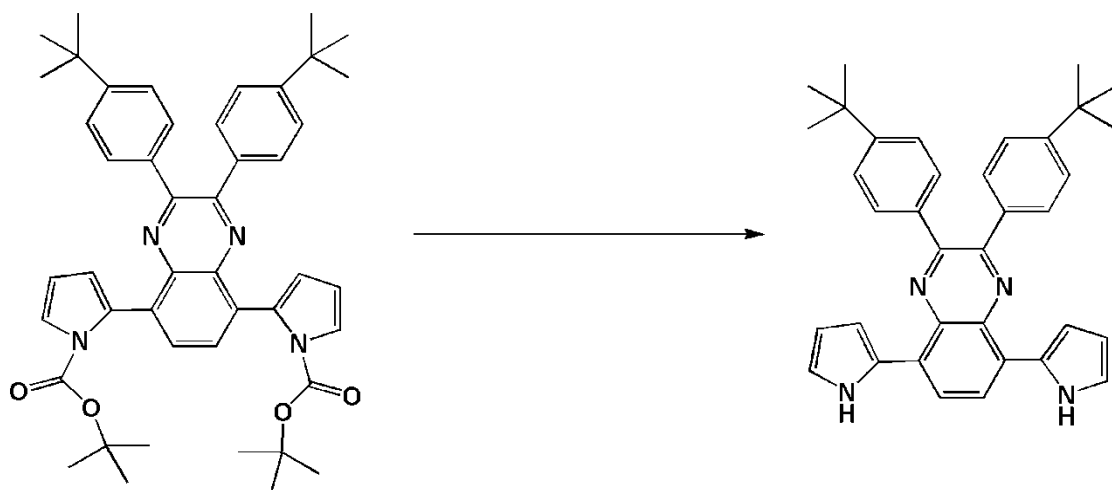


**Figure 2. 4 Schematic representation of deprotection reaction of TBPPQ**

### **2.3.2 Polymer Synthesis**

#### **2.3.2.1 Homopolymerization of TBPPQ**

The potentiodynamic electropolymerization of monomer on ITO was performed in a 0.1 M TBAPC and  $1 \times 10^{-2}$  M TBPPQ solution via applying potentials between 0.0 V and +1.0 V at a scan rate of 100 mV/s by multiple scan voltammetry. Due to the poor solubility of the monomer in acetonitrile (ACN), a mixture of ACN and dichloromethane (DCM) (95/5, v/v) was chosen as the solvent. The free standing homopolymers were washed with ACN in order to remove TBAPC and unreacted monomer after the electrolysis.

### 2.3.2.2 Copolymerization of TBPPQ with BiEDOT

BiEDOT was synthesized according to previously reported method [87] and the oxidative electrochemical copolymerization was achieved by repeated potential cycling in a solution containing BiEDOT and TBPPQ (w/w, 50:50) with 0.1 M TBAPC in ACN.

A structural representation of the reaction taking place during electrochemical copolymerization is shown in Figure 2.5.

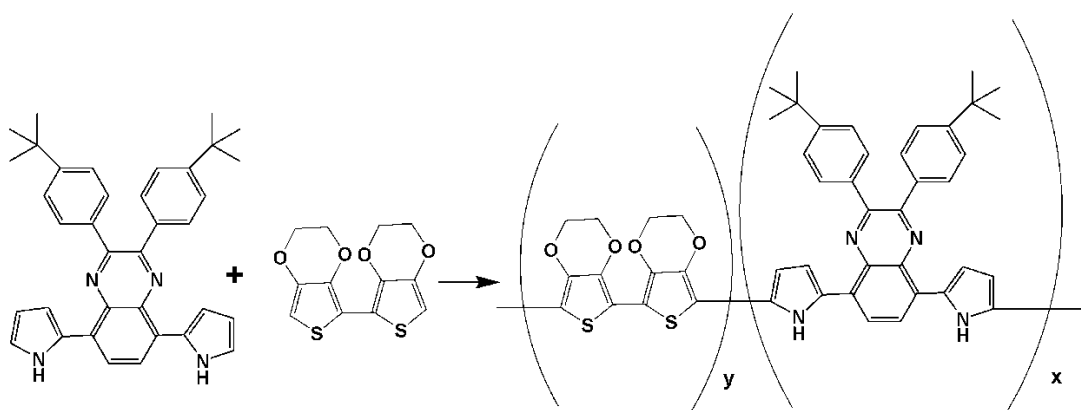


**Figure 2. 5 Schematic representation of copolymerization of TBPPQ and BiEDOT.**

### 2.3.2.3 Copolymerization of TBPPQ with BEBT

BEBT was synthesized according to previously reported method [70]. The potentiodynamic polymerization of TBPPQ with BEBT was carried out in a solution containing TBPPQ, BEBT and in 0.1 M TBAPC/ACN/DCM (95/5)

solvent–electrolyte couple by potentiodynamic runs between -0.1 and 0.9 V with a scan rate of 100 mV/s. After electrolysis, the film was washed with ACN to remove the supporting electrolyte and the unreacted monomer. A structural representation of the reaction taking place during electrochemical copolymerization is shown in Figure 2.6.

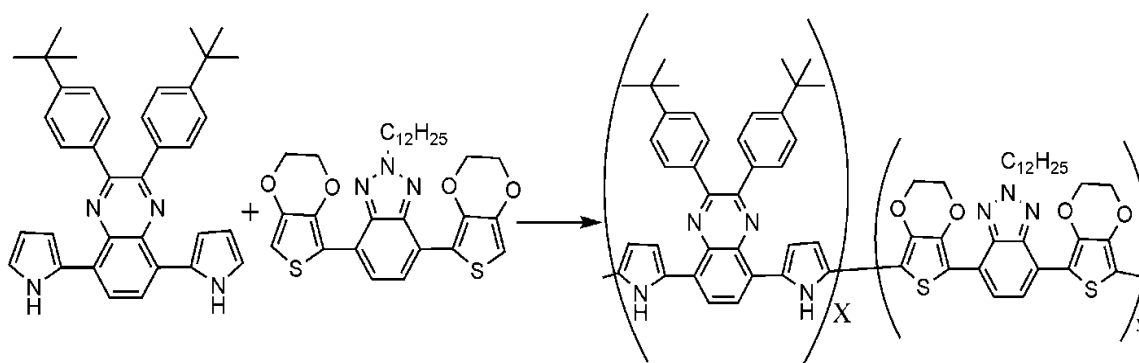


**Figure 2. 6 Schematic representation of copolymerization of TBPPQ and BEBT.**

## 2.4 Characterization of Polymer Films

### 2.4.1 Cyclic Voltammetry

The power of electrochemical methods that can be applied to the study of conducting polymer films deposited on a conducting surface is fairly broad and it has been thoroughly reviewed by Doblhofer et al. Among these methods, cyclic voltammetry (CV) has becoming increasingly popular as a mean to study redox states, due to its simplicity and versatility. Using CV, the electrode potential at



which a polymer undergoes reduction or oxidation can be rapidly located, information regarding the stability of the product during multiple redox cycles can be revealed. Since the rate of potential scan is variable, both fast and slow reactions can be followed. During a single experiment, CV has the ability to generate a new redox species at the first potential scan and then investigate the characteristic behaviors of species on the second and subsequent scans.

CV consists of linearly scanning the potential of a stationary working electrode using a triangular potential waveform (Figure 2.7. (a)). During the potential sweep, the potentiostat measures the current resulting from the applied potential. A typical CV investigation generally starts at low potentials where no redox reactions occur in anodic direction. After the electrode has reached sufficient potentials at which the monomer starts to get oxidized to a radical cation, anodic current starts to increase until the concentration of the monomer at the electrode surface approaches zero, which is signified by the formation of a peak. The intensity of the current starts to decay since the solution in the vicinity of the electrode has almost zero monomer concentration. The reduction of the deposited polymer is observed in the cathodic run. Upon consecutive cycling, a new oxidation peak appears due to the polymer. Due to increase in the active area of the working electrode owing to coating of an electroactive polymer on a metal electrode, there is an increase in the intensity of the current as the number of cycles increases. ( Figure 2.7. (b))

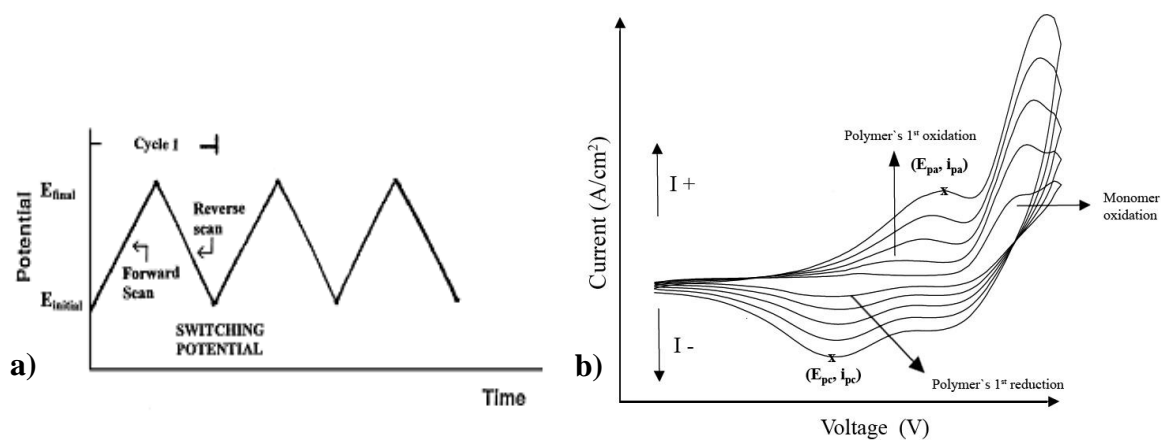


**Figure 2. 7 a) Typical Potential–Time excitation signal in CV b) CV of a representative type of electroactive monomer.**

The Randles-Sevcik equation states that the peak current is given by:

$$i_p = (2.69 \times 10^5) n^{3/2} A C D^{1/2} V^{1/2}$$

where  $n$  is the number of electrons,  $A$  is the surface area of the electrode (cm<sup>2</sup>),  $D$  is the diffusion constant (cm<sup>2</sup>/s),  $C$  is the bulk concentration of electroactive species (mol/cm<sup>3</sup>), and  $V$  is the scan rate (V/s). Therefore, for diffusion controlled system, the peak current is proportional to the square root of the scan rate. The rules change in electroactive polymer electrochemistry, when the polymer is adhered to the electrode surface. Hence, the process is not diffusion controlled,

and cannot be described by the Randles-Sevcik equation discussed above. Instead, the peak current for a surface bound species is given by the following equation:

$$i_p = n^2 F^2 \Gamma V / 4RT$$

where  $\Gamma$  is the concentration of surface bound electroactive centers ( $\text{mol}/\text{cm}^2$ ) and  $F$  is Faradays constant ( $96,485 \text{ C/mol}$ ). Thus, if a species is surface bound, both the anodic and cathodic peak current will scale linearly with scan rate. In a scan rate dependence experiment, the electroactive polymer is washed and placed in monomer- free electrolyte solution, and the polymer is then cycled between its oxidized and reduced forms at various scan rates while the  $i_p$  of both oxidation and reduction is monitored. If the  $i_p$  scales linearly with scan rate, then the process is said to be non-diffusion controlled, and the electroactive centers of the polymer are adhered to the electrode surface.

#### **2.4.2 Conductivity Measurements**

In order to determine the conductivity of polymer films, four probe conductivity measurements on the free standing films were performed. This method has several advantages for measuring electrical properties of conducting polymers over two probe method. First, the four probe technique eliminates errors caused by contact resistance, since two contacts measuring the voltage drop are different from the contacts applying the current across the sample. Secondly, this technique allows conductivity measurements over a broad range of applied currents. Furthermore, the four probe method allows for the contact points to be easily repositioned in various area of the film, thus allowing several conductivity measurements on the same sample. Figure 2.8 demonstrates a simple four-probe measurement setup.

Four equally spaced osmium tips touch the surface of polymer film taped on an insulating substrate. A known steady current is passed through the electrodes 1 and 4 and measured while the potential drop ( $\Delta V$ ) between contacts 2 and 3 assessed.

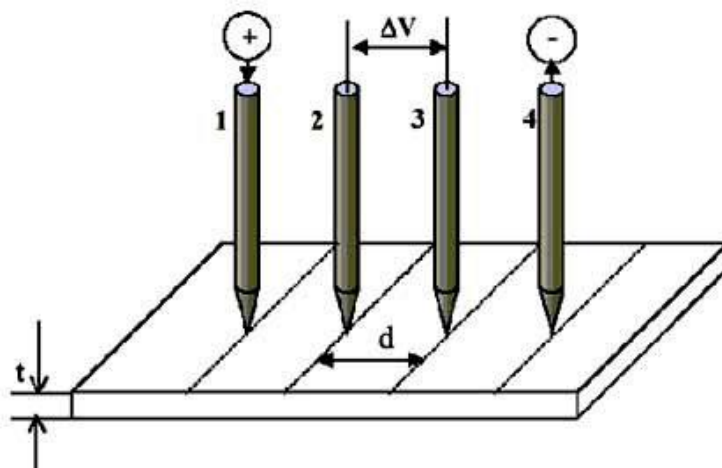


**Figure 2. 8 A simple four-probe measurement setup**

Conductivity is calculated from the following equation,

$$\sigma = \frac{\ln 2}{\pi R t}$$

where R is the resistance of the sample, and t is the thickness.

### 2.4.3 Spectroelectrochemistry

Spectroelectrochemistry is a combination of electrochemical and spectroscopic techniques that can be operated at the same time. Compared to common electrochemical methods, it can provide information on both electrochemical response and accompanying optical characteristics of all states of the electrochemical reaction. It is essential to gather information in-situ during electrochemical process. For the spectroelectrochemical studies, the polymer film coated ITO is placed in a cuvette that is equipped with a reference electrode and a Pt wire counter electrode. This cell is then connected to a potentiostat. The redox switching of conjugated polymers is accompanied by changes in electronic transitions. These electronic transitions can be probed with the use of UV-Vis spectroscopy. The polymer is stepwise oxidized while obtaining a spectrum at each potential. The results are then recorded as a graph of the extent of absorption as a function of wavelength. Spectroelectrochemistry experiments reveal key properties of conjugated polymers such as band gap ( $E_g$ ),  $\lambda_{\max}$ , the intergap states that appear upon doping and the evolution of polaron and bipolaron bands.

### 2.4.4 Switching Properties

For electrochromic applications, the significant point is the ability of a polymer to switch rapidly and exhibit a striking color change. Electrochromic switching studies can monitor absorbance changes with time during repeated potential stepping between bleached and colored states to obtain an insight into changes in the optical contrast (Figure 2.9). A square wave potential step method coupled with optical spectroscopy known as chronoabsorptometry is used to probe switching times and contrast in these polymers. Switching time is a time required for the polymer film to step between its oxidized and reduced states. In this study the potential is set at an initial value for a set period of time and is then stepped to a second potential for a set period of time before being switched back to the initial

potential. Electrochromic contrast is often reported as percent transmittance change ( $\Delta T$  %) at a specified wavelength where the material has the highest optical contrast.

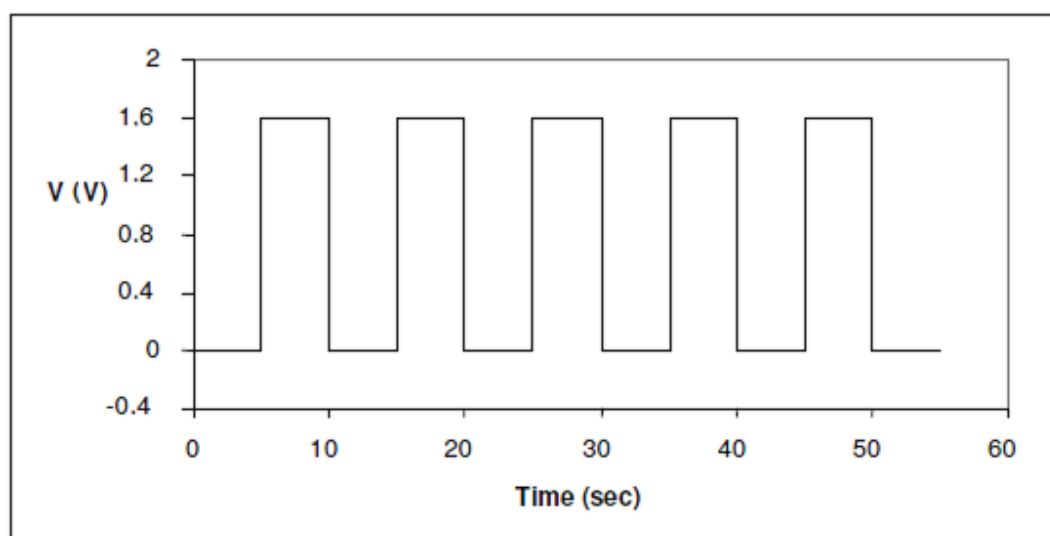


**Figure 2. 9 Square wave voltammetry**

#### **2.4.5 Colorimetry**

Colorimetry provides scientific means to define color. Rather than measuring the absorption bands, colorimetry measures the human eye's sensitivity to light across the visible region and graphically representing the track of doping-induced color changes of an electrochromic material or device. A commonly used scale that numerically defines colors has been established in 1931 by The Commission Internationale de l'Eclairage (CIE system) with  $L^*a^*b$ , CIE color spaces (Figure 2.10). Color measurements were performed via Coloreye XTH Spectrophotometer. This technique measures three values in relation to color: the

hue (dominant wavelength), which is the wavelength where maximum contrast occurs, saturation (purity), which is the color's intensity, and brightness (luminance).

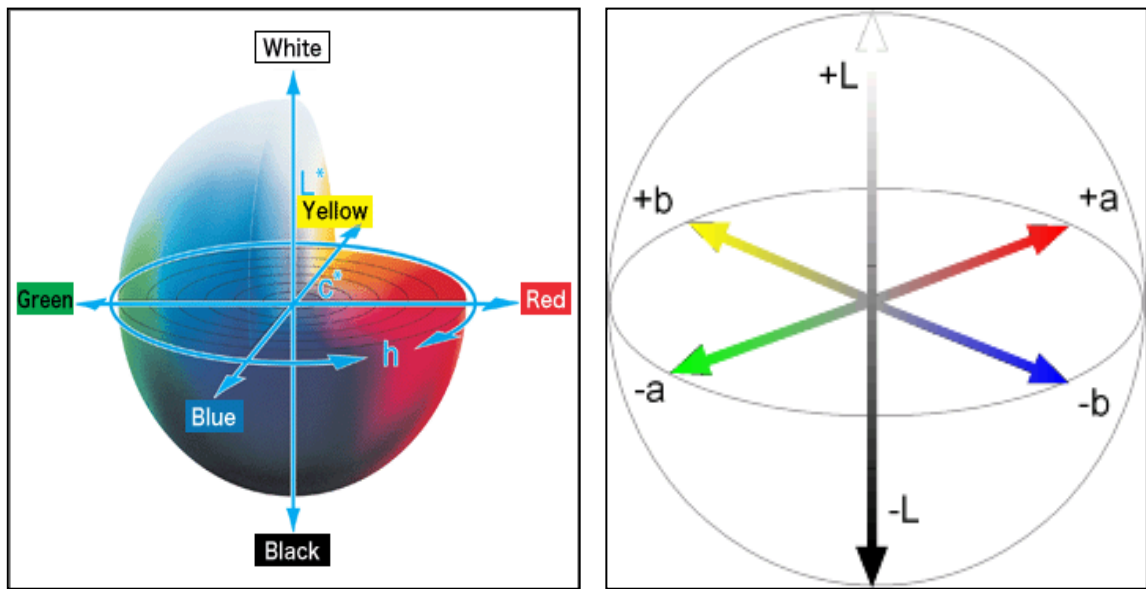


**Figure 2. 10 CIELAB color space**

## CHAPTER 3

### RESULTS AND DISCUSSION

#### 3.1 Characterization of the D-A-D Molecules

$^1\text{H}$ -NMR,  $^{13}\text{C}$ -NMR spectra of monomers were investigated in  $\text{CDCl}_3$  and chemical shifts ( $\delta$ ) were given relative to tetramethylsilane as the internal standard. Mass analyses were also performed for the characterization of monomers.

##### 3.1.1 2,3-bis(4-tert-butylphenyl)-5,8-dibromoquinoxaline (TBPB)

$^1\text{H}$ -NMR (400 MHz,  $\text{CDCl}_3$ ):  $\delta$  1.22 (s, 18 H), 7.27 (d, 4 H,  $J = 8.26$  Hz), 7.54 (d, 4 H,  $J = 8.30$  Hz), 7.72 (s, 2 H).  $^{13}\text{C}$ -NMR (100 MHz,  $\text{CDCl}_3$ ):  $\delta$  31.30, 34.81, 123.65, 125.31, 129.98, 130.13, 132.76, 135.25, 139.21, 152.90, 154.10, MS:  $m/e$  552 ( $\text{M}^+$ )



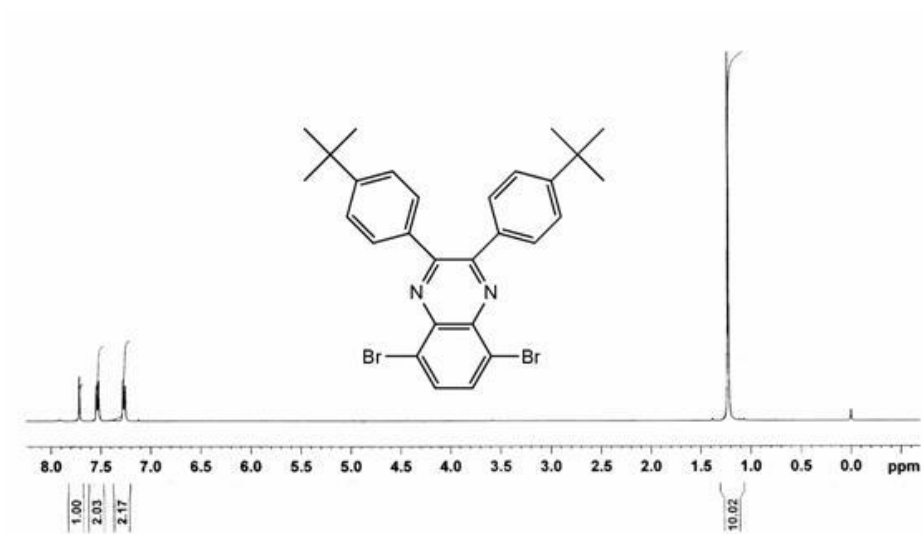


Figure 3.  $^1\text{H}$ -NMR spectrum of TBPB

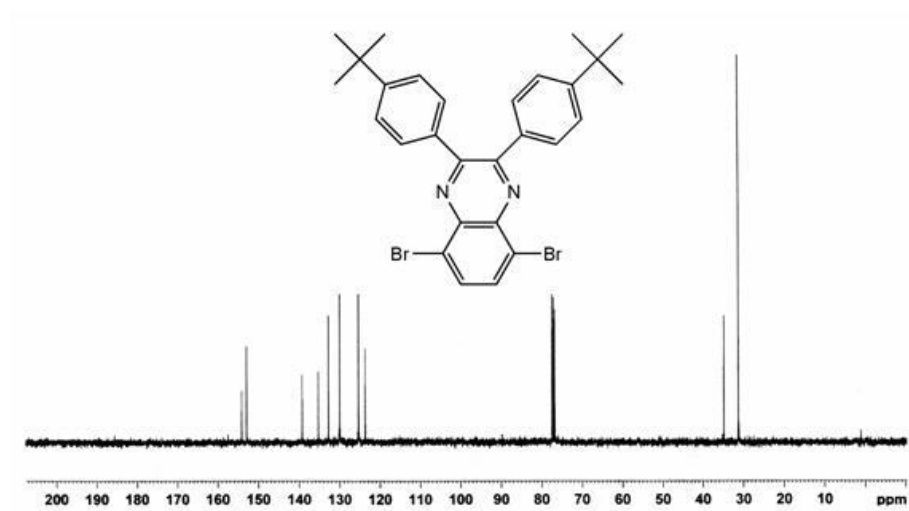


Figure 3.  $^{13}\text{C}$ -NMR spectrum of TBPB

### 3.1.2 5,8-Bis[N-(tert-butoxycarbonyl)-2-pyrrolyl]2,3-bis(4-tert-butylphenyl) quinoxaline

$^1\text{H}$ -NMR (400 MHz,  $\text{CDCl}_3$ ):  $\delta$  0.9 (s, 18 H), 1.22 (s, 18 H), 6.26 (t, 2 H,  $J=6.4$  Hz), 6.32 (d, 2 H,  $J=7.0$  Hz), 7.22 (d, 4 H,  $J = 8.8$  Hz), 7.43 (d, 4 H,  $J = 8.4$  Hz), 7.48 (q, 2 H,  $J=3$  Hz), 7.66 (s, 2 H).  $^{13}\text{C}$ -NMR (100 MHz,  $\text{CDCl}_3$ ):  $\delta$  27.2, 31.2, 34.7, 83.0, 110.4, 115.0, 123.0, 125.1, 128.0, 129.7, 131.5, 133.3, 136.1, 149.84, 151.2, 152.0.

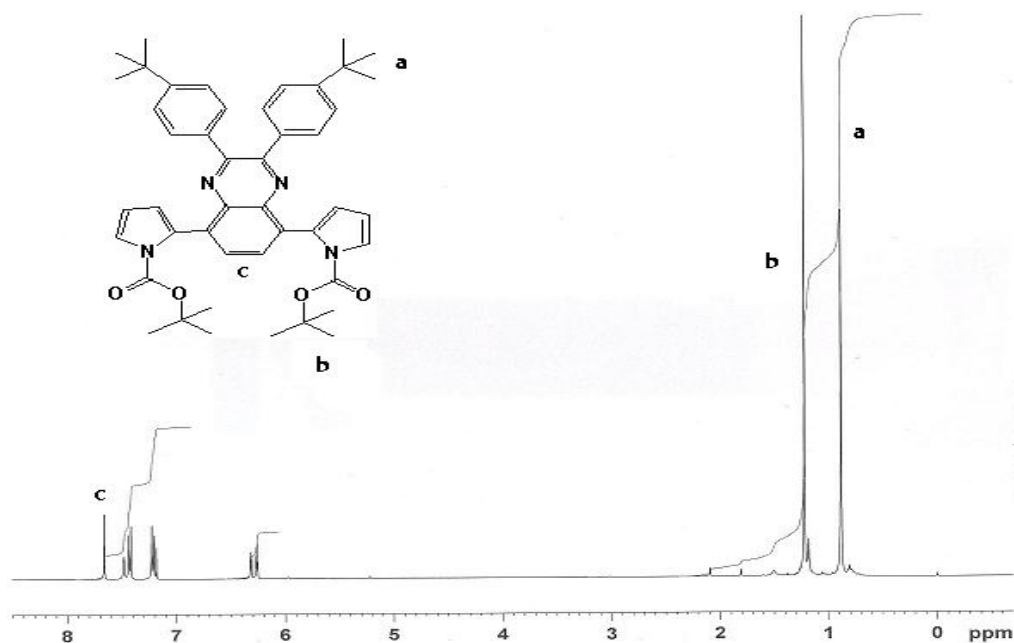
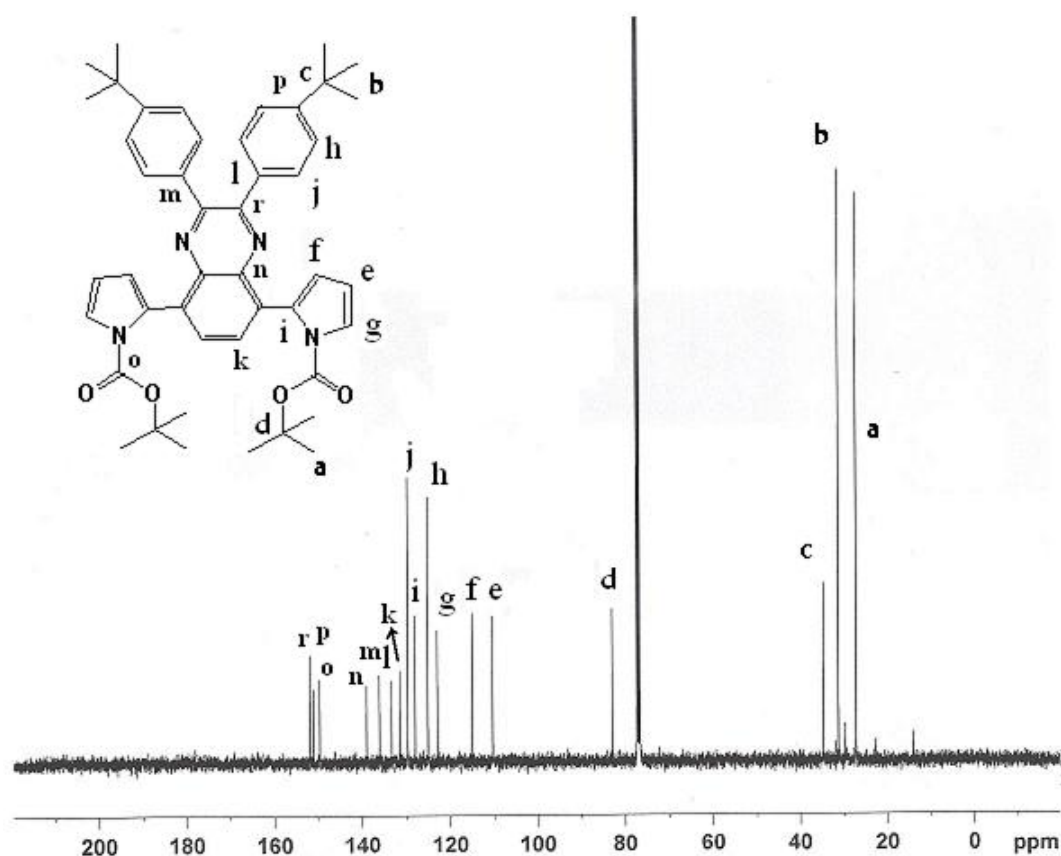


Figure 3.  $^1\text{H}$ -NMR spectrum of TBPEQ with t-boc



**Figure 3.**  $^{13}\text{C}$ -NMR spectrum of TBPPQ with t-boc

### 3.1.3 5,8-Bis [2-pyrrolyl] 2,3-bis(4-tert-butylphenyl)quinoxaline (TBPPQ)

$^1\text{H}$ -NMR (400 MHz,  $\text{CDCl}_3$ ):  $\delta$  1.31 (s, 18 H), 6.27 (m, 2 H), 6.82 (m, 2 H), 6.90 (m, 2 H) 7.35 (d, 4 H,  $J = 8.24$  Hz), 7.41 (d, 4 H,  $J = 8.22$  Hz), 8.00 (s, 2 H), 11.93 (s, 2 H).  $^{13}\text{C}$ -NMR (100 MHz,  $\text{CDCl}_3$ ):  $\delta$  31.6, 35.1, 107.7, 109.5, 119.7, 125.7, 125.8, 126.3, 129.7, 131.4, 136.4, 138.0, 151.4, 152.7, MS:  $m/e$  525 ( $\text{M}^+$ ).

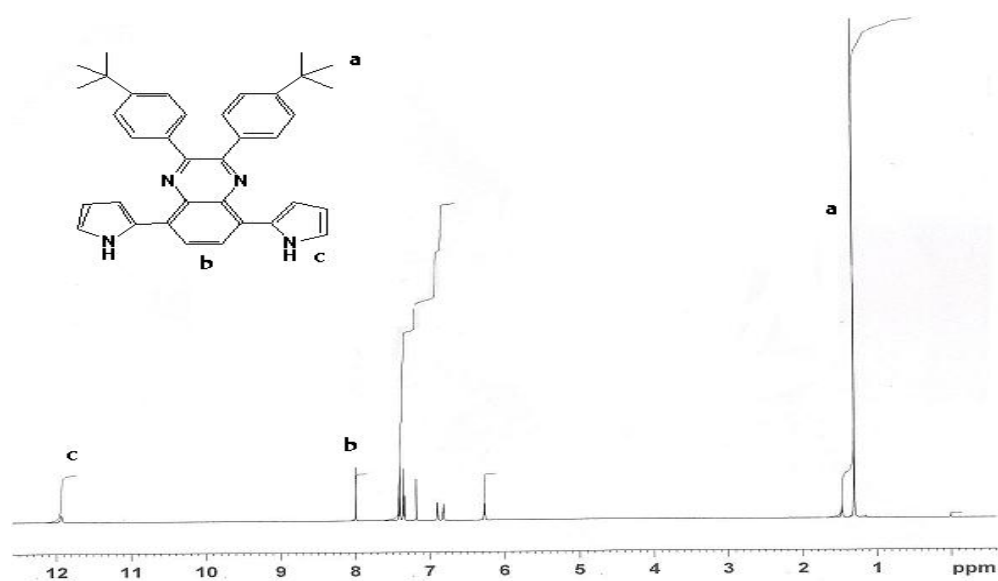


Figure 3. 5  $^1\text{H}$ -NMR spectrum of TBPPQ

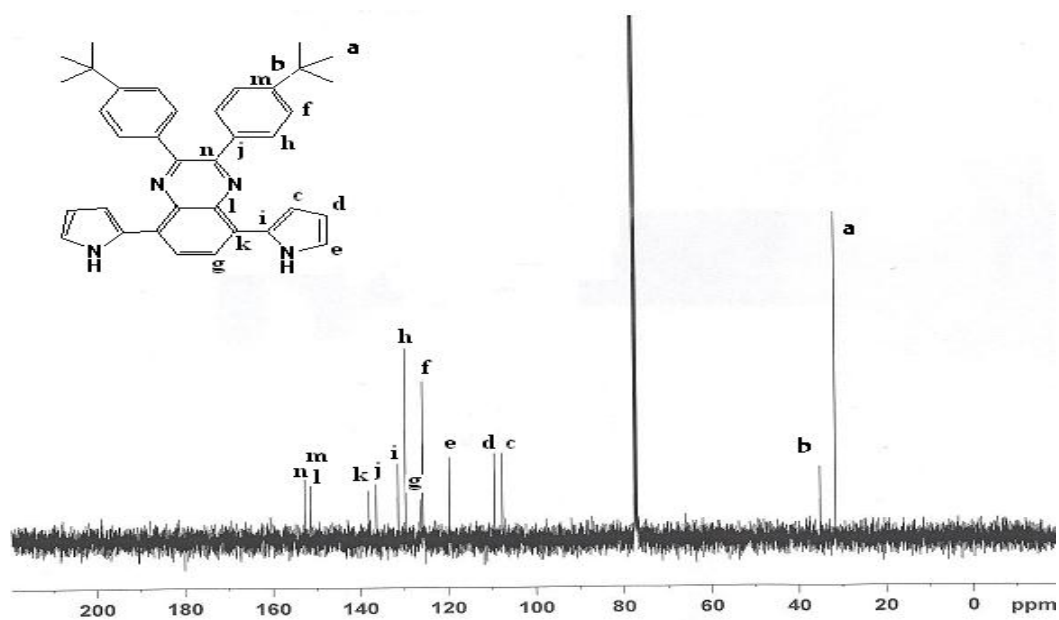


Figure 3. 6  $^{13}\text{C}$ -NMR spectrum of TBPPQ

### **3.2 Electrochemical and Electrochromic Properties of Donor-Acceptor-Donor Type Polymers**

#### **3.2.1 Electrochemical and Electrochromic Properties of Poly(2,3-bis(4-tert-butylphenyl)-5,8-di(1H-pyrrol-2-yl) quinoxaline) (PTBPPQ)**

##### **3.2.1.1 Electrochemistry of 2,3-bis(4-tert-butylphenyl)-5,8-di(1H-pyrrol-2-yl) quinoxaline (TBPPQ)**

The potentiodynamic electropolymerization of monomer on ITO was performed in a 0.1 M TBAPC and  $1 \times 10^{-2}$  M TBPPQ solution applying potentials between 0.0 V and +1.0 V at a scan rate of 100 mV/s via multiple scan voltammetry. Due to the poor solubility of the monomer in acetonitrile (ACN), a mixture of ACN and dichloromethane (DCM) (95/5, v/v) was chosen as the solvent.

The representative electrochemical growth revealing electroactivity of monomer TBPPQ and formation of corresponding insoluble polymer are given in Figure 3.7.

Polymerization was repeated on a Pt (1 cm x 1 cm) electrode to obtain a 20  $\mu$  thick free standing film for conductivity measurement ( $10^{-2}$  S/cm). The monomer oxidation potential was observed at 0.54 V (0.27 V vs Fc/Fc<sup>+</sup>), which is quite lower than the oxidation potential of pyrrole. This observation can be attributed to effective D–A match. After the first cycle, an oxidation peak at 0.23 V and its reverse cathodic peak at 0.13 V appeared. These values are also quite lower than those for polypyrrole. After subsequent runs electroactivity increases with increasing scan number. The peak at 0.54 V decreases as a result of monomer consumption in the diffusion layer. A direct relation between current response and scan rate was observed for polymer film which proved that the film was well adhered on the electrode surface and electroactive (Figure 3.8). TBPPQ was

coated on Pt wire potentiodynamically over 40 cycles from a 0.01 M monomer and 0.1 M TBAPC DCM/ACN (5/95, v/v) solution. Anodic and cathodic peak currents revealed a linear relationship as a function of scan rate for polymer film, indicating that electrochemical processes are not diffusion limited and reversible even at high scan rates [88,89].

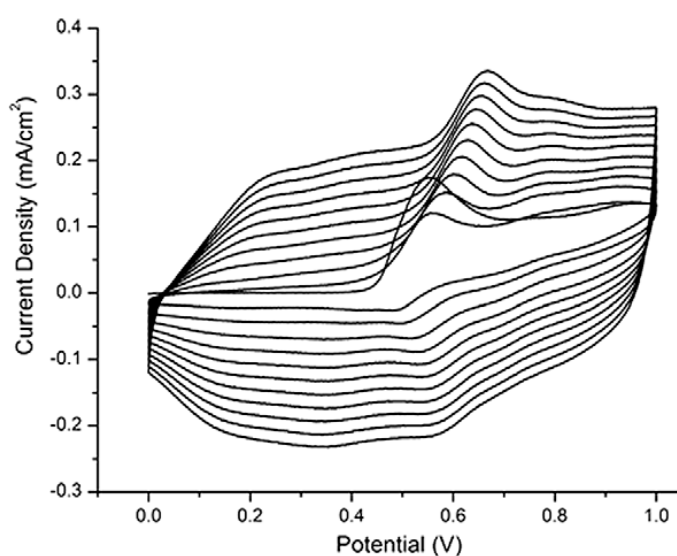


**Figure 3. 7 Repeated potential scan electropolymerization of TBPPQ ( $10^{-2}$  M) at 100 mV/s in 0.1 M TBAPC in DCM/ACN (5/95, v/v) on ITO electrode vs Ag wire after 40 cycles**

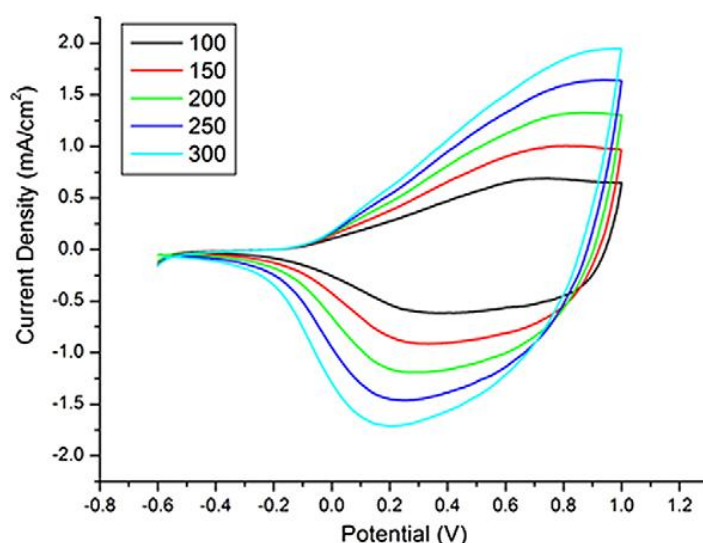


**Figure 3. 8 Scan rate dependence of PTBPPQ film on Pt vs Ag wire in 0.1 M TBAPC/ACN (a) 100, (b) 150, (c) 200, (d) 250, (e) 300 mV/s**

### **3.2.1.2 Spectroelectrochemistry of Poly(2,3-bis(4-tert-butylphenyl)-5,8-di(1H-pyrrol-2-yl) quinoxaline) (PTBPPQ)**

Spectroelectrochemical studies were performed in order to monitor in situ optical changes upon doping. Spectral changes were recorded by UV–Vis–NIR spectrophotometer in a monomer free, 0.1 M TBAPC/ACN solution while varying the applied potential between -0.5 V and +1.1 V. Generally, donor acceptor type polymers show two distinct absorption maxima due to high energy and low energy  $\pi$ - $\pi^*$  transitions [90]. As a donor acceptor polymer, PTBPPQ showed these absorption maxima due to the transitions from pyrrole based valence band to its antibonding counterpart as well as to the substituent localization narrow conduction band [77]. In order to achieve green color these absorption bands should be observed in the visible region at around 400 nm and

700 nm. PTBPPQ showed  $\pi$ - $\pi^*$  transitions centered at 408 nm and 745 nm. As doping proceeds, formation of charge carriers leads to new absorption bands at 1100 nm and 1480 nm while absorptions for the neutral state are decreasing. This change represents the formation of polaron and bipolaron bands respectively [91].

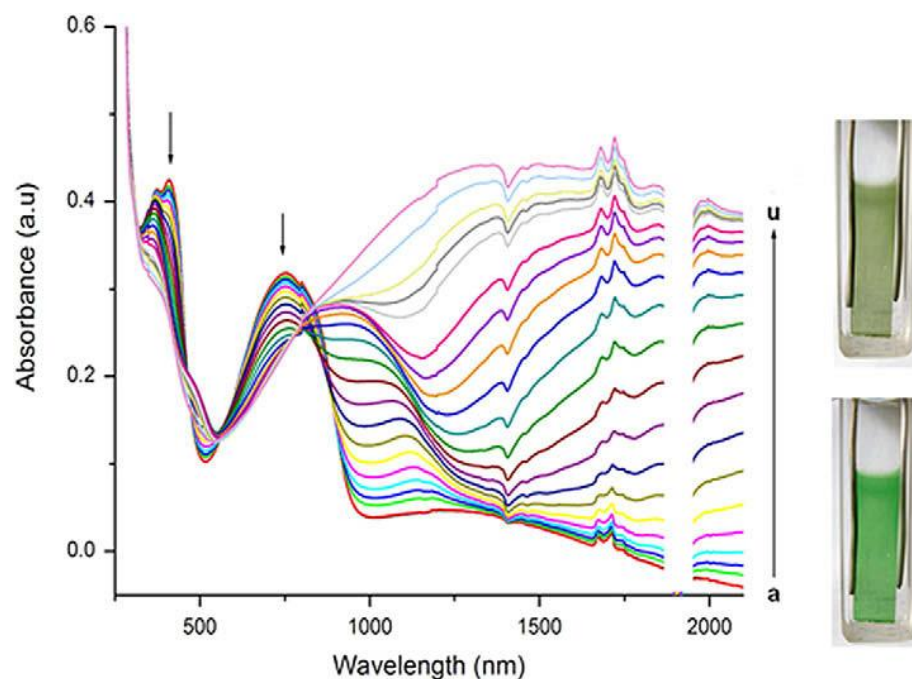


**Figure 3. 9 Spectroelectrochemistry of PTBPPQ film on ITO-coated glass slide in a monomer free, 0.1 M TBAPC/ACN electrolyte–solvent couple at applied potentials (V) vs Ag wire: (a)  $-0.5$ , (b)  $-0.4$ , (c)  $-0.3$ , (d)  $-0.2$ , (e)  $-0.1$ , (f)  $0.0$ , (g)  $0.1$ , (h)  $0.15$ , (i)  $0.2$ , (j)  $0.25$ , (k)  $0.3$ , (l)  $0.35$ , (m)  $0.4$ , (n)  $0.45$ , (o)  $0.5$ , (p)  $0.6$ , (q)  $0.7$ , (r)  $0.8$ , (s)  $0.9$ , (t)  $1.0$ , and (u)  $1.1$**



The band gap of the polymer is 1.25 eV which was calculated from the onset of the second  $\pi$ - $\pi^*$  transition. This value is in good agreement with values reported for the polymers having the same acceptor unit, with EDOT and 3-hexylthiophene as the donor units (PTBPEQ: 1.18 eV and PHTQ: 1.75 eV) [92,93]. Spectroelectrochemical studies for the polymer film showed that the color of the film changed from saturated green (Y:464, x:0.301, y:0.401) to brownish green (Y:492, x:0.309, y:0.358) during oxidation (Figure 3.9). Y refers to L, x refers to a, y refers to b in CIE system. Coloration efficiency is the ratio between the injected/ejected charge per unit area of the electrode and the change in the optical density at a dominant wavelength. Coloration efficiency of the PTBPPQ was found to be 85 cm<sup>2</sup> C<sup>-1</sup> at 100 % full switch at 408 nm.

### **3.2.1.3 Electrochromic switching of Poly(2,3-bis(4-tert-butylphenyl)-5,8-di(1H-pyrrol-2-yl) quinoxaline) (PTBPPQ)**

In order to determine switching time and percent transmittance change ( $\Delta T\%$ ) of the polymer between neutral and oxidized states, it was polymerized on ITO coated glass slides. The polymer film was stepped between -0.5 V and 1.1 V with a switching interval of 5 s in 0.1 M TBAPC/ACN while recording percent transmittance as a function of time (Figure 3.10, Figure 3.11, Figure 3.12). PTBPPQ film showed a 21 % optical contrast at 408 nm and a 12 % optical contrast at 745 nm. In the NIR region it showed a remarkable contrast of 65 % which confirmed that it can be used for near-IR applications. A square-wave potential step method was used to calculate the switching time. The polymer achieved 95 % of its optical contrast in 0.6 s at 408 nm. At 745 nm, which corresponds to the second  $\pi$ - $\pi^*$  transition, the switching time was recorded as 0.3 s. In the near-IR region (1480 nm), polymer film showed a remarkably fast switching time of less than 0.2 s [94–96] (Table 3.1). Kinetic studies for polymer

film showed that PTBPPQ has not only a comparable optical contrast, but also faster switching times compared to its competitors, PTBPEQ [92] and PHTQ [93].

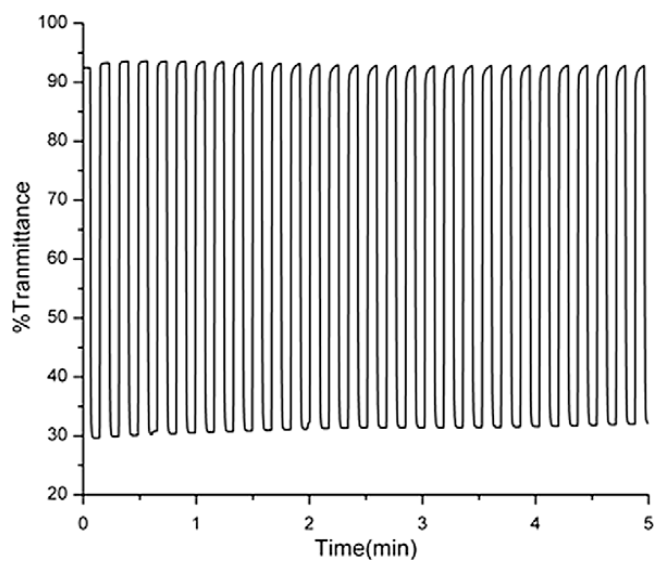


**Figure 3. 10 Electrochromic switching, percent transmittance change monitored at 1480 nm for PTBPPQ in 0.1 M TBAPC/ACN**

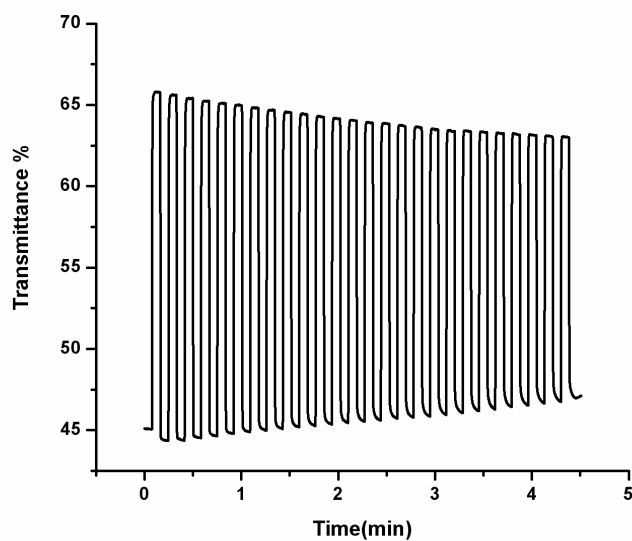


**Figure 3. 11 Electrochromic switching, percent transmittance change monitored at 408 nm for PTBPPQ in 0.1 M TBAPC/ACN**

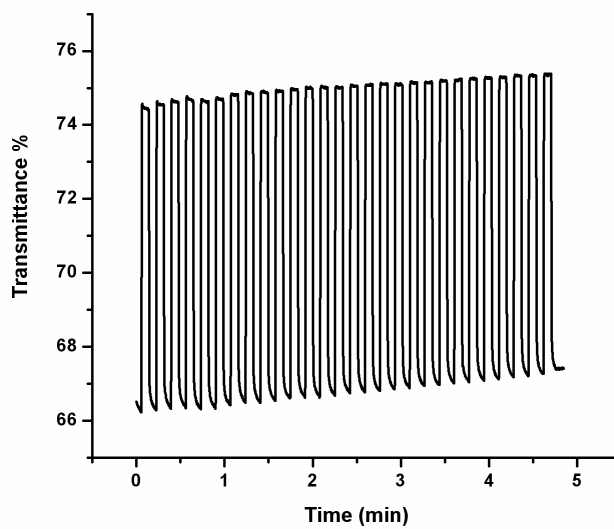


**Figure 3. 12 Electrochromic switching, percent transmittance change monitored at 745 nm for PTBPPQ in 0.1 M TBAPC/ACN**

**Table 3.1 Optical contrasts and related switching times of TBPPQ**

$\lambda_{\text{max}}$	408 nm	745 nm	1480 nm
Optical contrast	21 %	12 %	65 %
Switching Time	0.6 sec	0.3 sec	0.1 sec

**3.2.2 Electrochemical and Electrochromic Properties of Poly(2,3-bis(4-tert-butylphenyl)-5,8-di(1H-pyrrol-2-yl) quinoxaline-co-bi-etylenedioxy thiophene) P(TBPPQ-co-BiEDOT)**

**3.2.2.1 Electrocrochemistry of Poly(2,3-bis(4-tert-butylphenyl)-5,8-di(1H-pyrrol-2-yl) quinoxaline-co-bi-etylenedioxy thiophene) P(TBPPQ-co-BiEDOT)**

Copolymerization is a facile method to observe interesting combinations of the properties observed in the corresponding homopolymers and to enhance its optical properties [97-99]. In copolymerization reactions, the two monomers having close oxidation potentials should be chosen in order to achieve an effective electrochemical reaction. In this manner BiEDOT was chosen due to its oxidation potential ( $E_a$ , BiEDOT =  $\sim +0.6$  V,  $E_a$ , TBPPQ of + 0.54 V vs Ag wire) and superior optical and mechanical properties [100]. The oxidation/reduction

behavior of copolymer was investigated by CV in TBAPC (0.1 M)/ACN/DCM solvent-electrolyte couple. Experiments were carried out in an electrolysis cell equipped with indium doped tin oxide (ITO) coated glass plate as the working, Pt wire counter and Ag wire reference electrodes. After electrolysis, the films were washed with ACN to remove the supporting electrolyte and the unreacted monomers. To investigate the CV behavior of the copolymer, we performed CV studies for BiEDOT under the same experimental conditions (Figure 3.13). Figure 3.13 also shows the cyclic voltammogram of P(TBPPQ-co-BiEDOT) performed between -0.1 and 1.2 V at a scan rate of 100 mV s<sup>-1</sup>. The first cycle represents both the oxidation of TBPPQ and BiEDOT respectively. As the number of cycles increased, new anodic (0.40 V) and cathodic (0.02 V) peaks were observed due to the evolution of the copolymer on the electrode. There was a drastic change in the voltammogram; both the current increase between consecutive cycles and the oxidation potential of the material were different than those of TBPPQ and BiEDOT, which, in fact, could be interpreted as the formation of copolymer. The effect of scan rate on the copolymer film was also investigated. Results showed a linear relationship between the peak current and the scan rate which indicates the presence of an electroactive polymer film which is well adhered on the electrode and the redox processes were nondiffusion controlled (Figure 3.17).

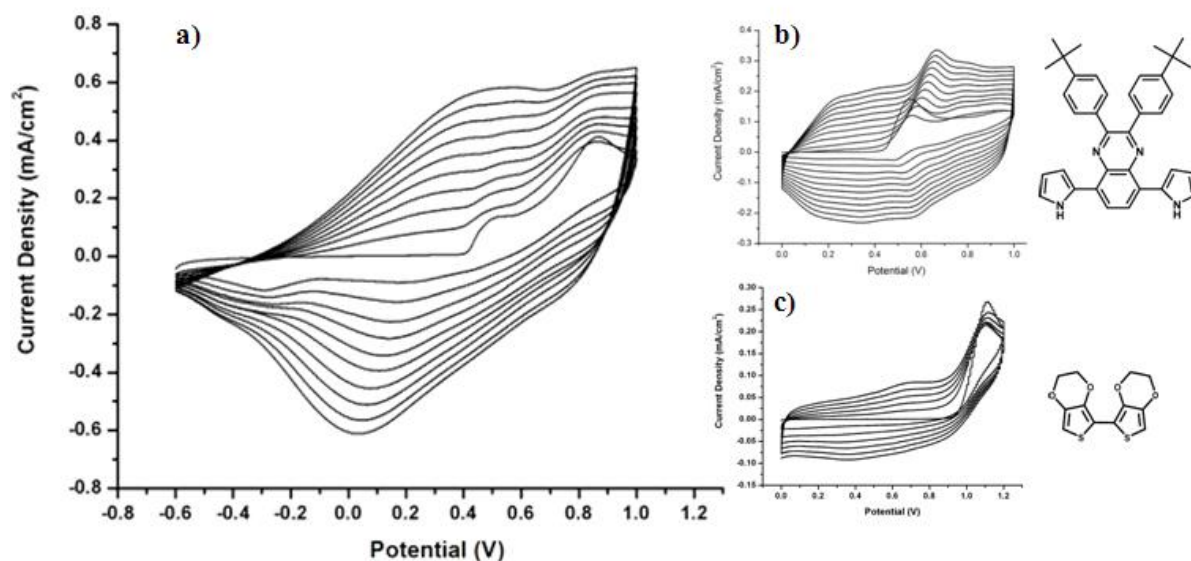


**Figure 3. 13 Cyclic voltammetry of a) P(TBPPQ-co-BiEDOT) b) TBPPQ c) BiEDOT in 0.1M TBAPC/ACN/DCM at scan rate of 100 mV/s**

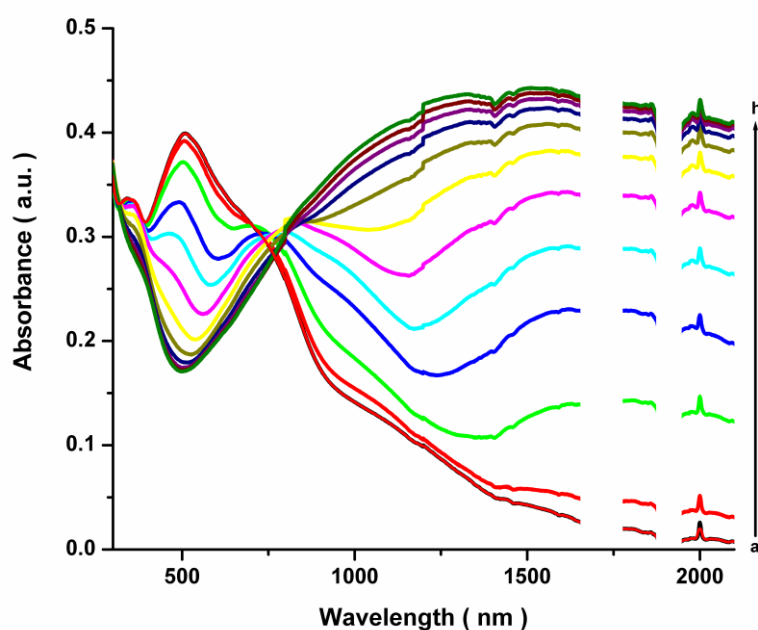
### 3.2.2.2 Spectroelectrochemistry of Poly(2,3-bis(4-tert-butylphenyl)-5,8-di(1H-pyrrol-2-yl) quinoxaline-co-bi-etylenedioxy thiophene) P(TBPPQ-co-BiEDOT)

Spectroelectrochemical analysis of the copolymer was studied in order to find the most compelling evidence for electrochemical copolymerization and to elucidate electronic transitions upon doping–dedoping of the polymer. To do this, copolymer was electrosynthesized onto ITO electrodes under the same experimental conditions (-0.6V and +1.0V in ACN/TBAPC (0.1 M) solution) used for the cyclic voltammetry studies. Later the ITO electrode was transferred into cuvettes containing monomer free electrolyte solution. Spectroelectrochemistry study was probed by a UV-Vis-NIR spectrophotometer

with gradual increase of the applied potential between -0.5 and 0.9 V. Generally, p-doping conducting polymers display formation of new charge carrier bands upon oxidation. That results in a decay in the intensity of  $\pi$ - $\pi^*$  transition and formation of the new spectral features at longer wavelengths.

Figure 3.9 presents the spectroelectrochemistry of PTBPPQ revealing  $\pi$ - $\pi^*$  transition in the neutral state which fades upon increasing the applied voltage. The electronic band gap, defined as the onset energy for the  $\pi$ - $\pi^*$  transition, was found to be 1.25 eV (408 and 745 nm). The polymer displayed light green (x: 0.309, y: 0.358, Y:492) and green (x: 0.301, y: 0.401, Y:464) color in its neutral and doped states. Assessment of the spectroelectrochemical behavior of the copolymer and the evaluation of the differences of the spectral signatures of the material to those of the respective homopolymers reveal the most compelling evidence of copolymerization. At neutral state,  $\lambda_{\text{max}}$  (due to the broad  $\pi$ - $\pi^*$  transition of the copolymer) was found to be 510 nm and  $E_g$  was calculated as 1.12 eV by inserting the onset wavelength on de-Broglie equation. The optical properties of PBiEDOT have been thoroughly investigated in the literature. PBiEDOT reveals  $\pi$ - $\pi^*$  transition centered at 587 nm and has a band gap of 1.6 eV. Thus,  $\lambda_{\text{max}}$  and  $E_g$  of the copolymer are considered to be in agreement with the expectations compared to parent polymers.  $\lambda_{\text{max}}$  for the copolymer is between those of the PBiEDOT and the homopolymer. As seen from the table, introduction of BiEDOT to the polymer chain led to a tremendous decrease in the band gap. These numerical values also support the copolymerization phenomenon. At 0.4 V copolymer presents a weakened (and shifted)  $\pi$ - $\pi^*$  transition at 510 nm and yet a new transition around 1320 nm originates due to the charge carrier bands. Further doping resulted in the further shift of  $\lambda_{\text{max}}$  along with decay in its intensity (Figure 3.14). Potentials beyond 0.7 V enhanced the formation of bipolaron bands signified by the broad transition beyond 1000 nm. Hence, doping of the copolymer not only results in a decrease in the intensity of  $\pi$ - $\pi^*$  transition (which





is due to increase in conjugation length and the influence of high electron density resulting from the incorporation of BiEDOT units) but also a decrease in the peak width with a shift in  $\lambda_{\text{max}}$ , all of which has a significant effect on displayed color. This particular trend clarifies the underlying reason of perceived distinct multichromism where the polymer displayed purple, gray, light green, and transmissive blue color at -0.5, 0.4, 0.6, 1.0 V, respectively. The colors of the electrochromic materials were determined by performing colorimetry measurements. CIE system was used as the quantitative scale to define the colors. There attributes of color; hue ( $a$ ), saturation ( $b$ ) and luminance ( $L$ ) were measured in situ at the fully oxidized and the fully reduced states in addition to states in between and the results were recorded in Table 3.2.



**Figure 3. 14 Spectroelectrochemistry of P(TBPPQ-co-BiEDOT) as a function of applied potential between -0.5 and 0.9 V in 0.1 M TBAPC/ACN: (a) -0.5, (b) -0.8, (c) -0.6, (d) -0.4, (e) -0.2, (f) 0.0, (g) +0.4, (h) 0.9 V vs Ag wire**



**Table 3.2 Electrochromic Properties of TBPPQ-co-BiEDOT**

<b>Colors</b>												
	<b>Purple</b>			<b>Grey</b>			<b>Light Green</b>			<b>Transmissive Blue</b>		
	<b>Y</b>	<b>x</b>	<b>y</b>	<b>Y</b>	<b>X</b>	<b>Y</b>	<b>Y</b>	<b>X</b>	<b>Y</b>	<b>Y</b>	<b>x</b>	<b>y</b>
<b>Copolymer</b>	<b>141</b>	<b>0.30</b>	<b>0.26</b>	<b>532</b>	<b>0.31</b>	<b>0.33</b>	<b>622</b>	<b>0.31</b>	<b>0.36</b>	<b>652</b>	<b>0.29</b>	<b>0.33</b>

### 3.2.2.3 Electrochromic switching of Poly(2,3-bis(4-tert-butylphenyl)-5,8-di(1H-pyrrol-2-yl) quinoxaline-co-bi-ethylenedioxy thiophene) P(TBPPQ-co-BiEDOT)

Electrochromic switching studies were performed to test the ability of a polymer to switch rapidly and the ability to exhibit striking color change. The experiments carried out by spectroelectrochemistry showed the ability of P(TBPPQ-co-BiEDOT) to switch between its neutral and doped states with a change in

transmittance at a fixed wavelength. During the experiment, the percent transmittance ( $T\%$ ) of the polymer was measured using a UV–Vis spectrophotometer at 510 nm. The polymer film was synthesized on ITO-coated glass slides in 0.1 M TBAPC in ACN. In this double potential step experiment for P(TBPPQ-co-BiEDOT), the potential was set at an initial value (-0.2 V) for a set period of time (5s) and was stepped to a second potential (+1.0 V) for the same period of time, before being switched back to the initial potential again (Figure 3.15). Electrochromic contrast was reported as a percent transmittance change ( $\Delta T\%$ ) at 1320 nm where the electrochromic material has the highest optical contrast. The contrast was measured as the difference between  $T\%$  in the reduced and oxidized forms and  $\Delta T\%$  was noted as 57 %. Results showed that time required to reach 95 % of ultimate  $\Delta T\%$  was 2.4 s. At 510 nm, 23 % transmittance change was recorded with 1.2 s switching time (Table 3.3). Copolymer revealed reasonable stability and higher optical contrast as 23 % in the visible region (optical contrasts of homopolymer at 408 nm and 745 nm are 21 % and 12 % respectively). Hence, the copolymerization was found to enhance the optical contrast at the expense of the increase in switching time (switching time of homopolymer was found to be 0.6 s, 0.3 s and 0.1 s at related wavelengths).

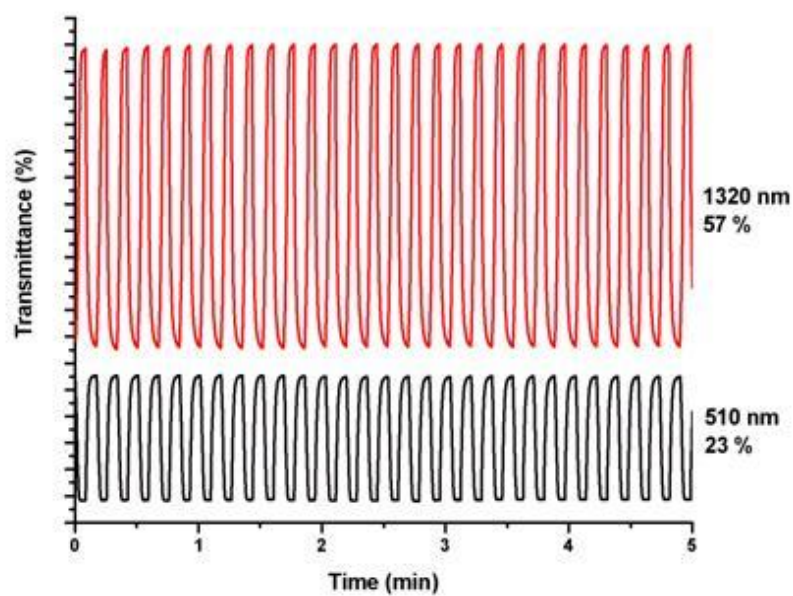


**Figure 3. 15 Electrochromic switching, optical absorbance change monitored at 510 nm and 1320 nm for P(TBPPQ-co-BiEDOT) in 0.1 M TBAPC/ACN**

**Table 3.3 Optical Contrasts and Related Switching Times of P(TBPPQ-co-BiEDOT)**

$\lambda_{\text{max}}$	510 nm	1320 nm
Optical contrast	23 %	57 %
Switching Time	1.2 sec	2.4 sec

### **3.2.3 Electrochemical and Electrochromic Properties of Poly(2,3-bis(4-tert-butylphenyl)-5,8-di(1H-pyrrol-2-yl)quinoxaline-co-4,7-bis(2,3-dihydrothieno [3,4-b][1,4]dioxin-5-yl)-2-dodecyl-2H-benzo[1,2,3] triazole) P(TBPPQ-co-BEBT)**

#### **3.2.3.1 Electrochemistry of Poly(2,3-bis(4-tert-butylphenyl)-5,8-di(1H-pyrrol-2-yl) quinoxaline-co-4,7-bis(2,3-dihydrothieno[3,4-b][1,4]dioxin-5-yl)-2-dodecyl-2H-benzo [1,2,3] triazole) P(TBPPQ-co-BEBT)**

The oxidation/reduction behavior of copolymer was investigated by CV using same experimental conditions used for the copolymerizations with BiEDOT (0.1M TBAPC/ACN/DCM at scan rate of 100 mV/s ). Experiments were carried out in an electrolysis cell equipped with indium doped tin oxide (ITO) coated glass plate as the working, Pt wire counter and Ag/ wire reference electrodes. Figure 3.16 represents the electropolymerization of BEBT, TBPPQ and copolymer for comparison. As seen, during polymerization two separate monomer peaks were observed due to oxidation of both TBPPQ (at 0.54 V) and BEBT (at 0.97 V) which lead to copolymerization on the electrode surface. The resulting copolymer has an oxidation potential of 0.40 V and a reversible reduction couple at 0.05 V. Copolymer with BEBT can be doped and dedoped at very similar potentials to the copolymer with BiEDOT. Although BiEDOT and BEBT have different oxidation potentials, the resulting copolymers have very similar redox behaviors. There was a drastic change in the voltammogram both the current increase between consecutive cycles and the oxidation potential of the material were different than those of TBPPQ and BEBT (Figure 3.16), which, in fact, could be interpreted as the formation of copolymer. The effect of scan rate variation on the copolymer film was also investigated. Results showed a linear relationship between the peak current and the scan rate exists which indicates the

presence of an electroactive polymer film which is well adhered on the electrode and charge transfer process was not dominated by diffusion (Figure 3.17).

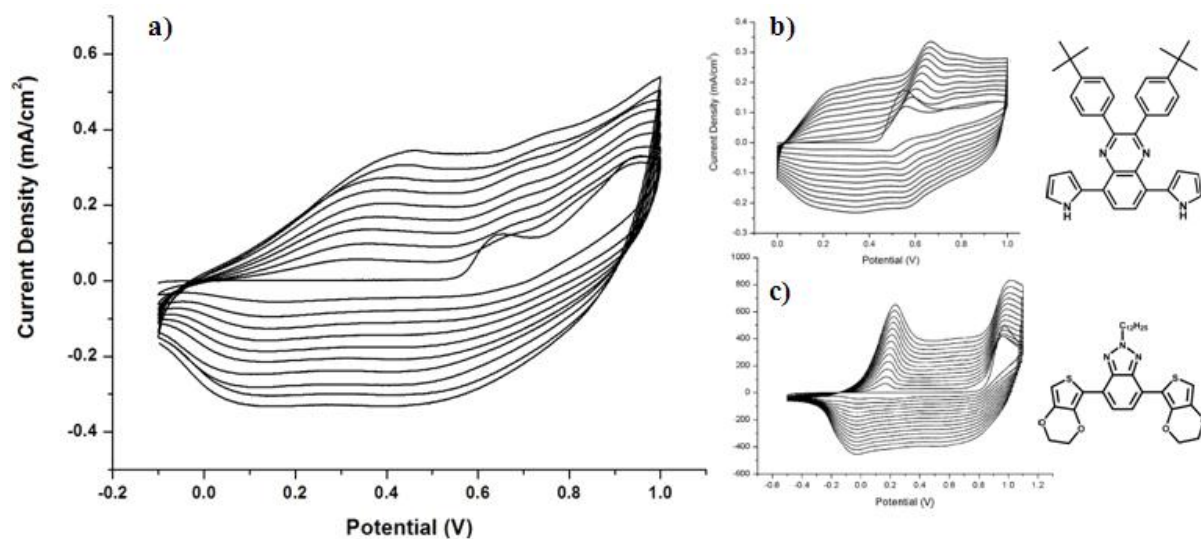


**Figure 3. 16 Cyclic voltammetry of a) P(TBPPQ-co-BEBT) b) TBPPQ c) BEBT in 0.1M TBAPC/ACN/DCM at scan rate of 100 mV/s**

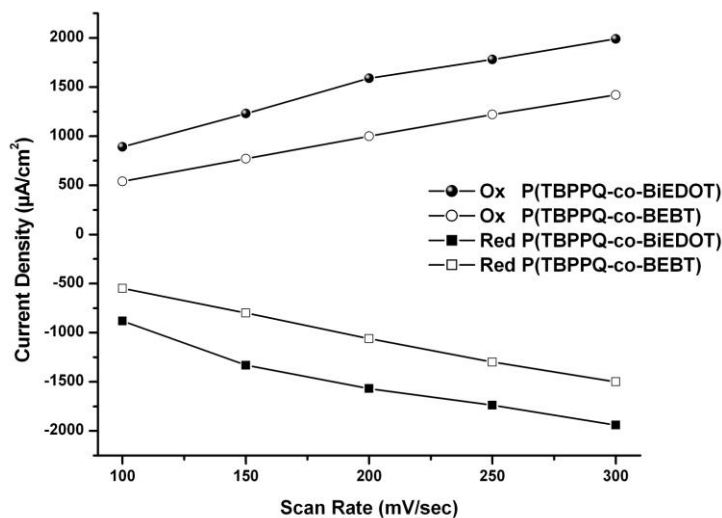


**Figure 3. 17 Linear relationship between scan rate and peak current of P(TBPPQ-co-BiEDOT) and P(TBPPQ-co-BEBT) films in monomer free, 0.1M TBAPC/ACN solution**

### 3.2.3.2 Spectroelectrochemistry of Poly(2,3-bis(4-tert-butylphenyl)-5,8-di(1H-pyrrol-2-yl) quinoxaline-co-4,7-bis(2,3-dihydrothieno[3,4-b][1,4]dioxin-5-yl)-2-dodecyl-2H-benzo [1,2,3] triazole) P(TBPPQ-co-BEBT)

For the spectroelectrochemistry of the copolymer, the film was deposited on ITO via potentiostatic electrochemical polymerization of TBPPQ (0.01 M) in the presence of BEBT and 0.1M TBAPC/ACN while the potential was swept between -0.1 V and +0.9 V. P(TBPPQ-co-BEBT) coated ITO was investigated by UV-Vis

spectroscopy in monomer free electrolytic system by switching the potential between -0.5 V and +0.9 V.

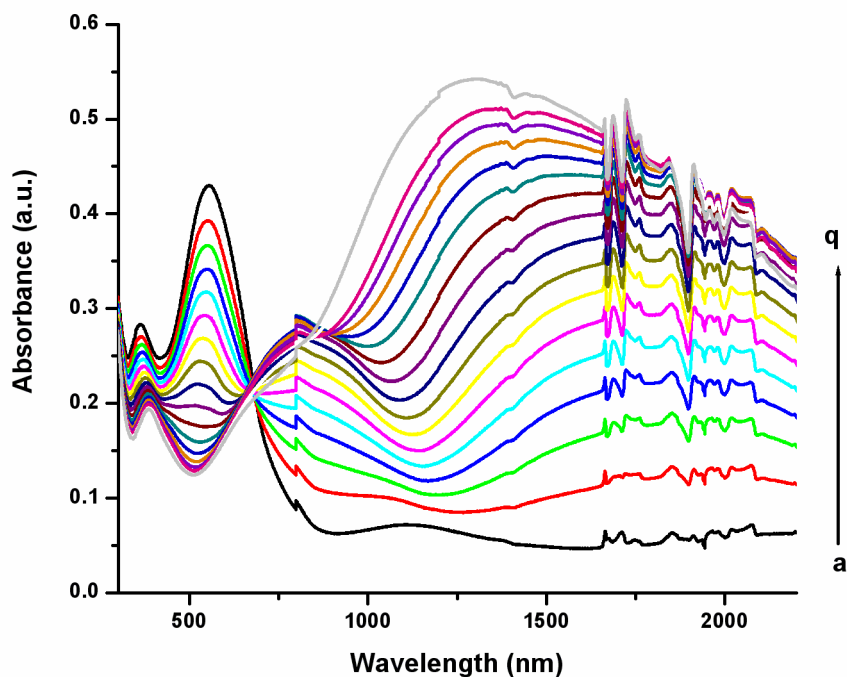


**Figure 3. 18 Spectroelectrochemistry of P(TBPPQ-co-BEBT) as a function of applied potential between -0.5 and 0.9 V in 0.1 M TBAPC/ACN : (a) -0.5, (b) -0.4, (c) 0.0, (d) 0.1, (e) 0.2, (f) 0.3, (g) 0.35, (h) 0.4, (i) 0.45, (j) 0.5, (k) 0.55 (l) 0.6, (m) 0.65, (n) 0.7, (o) 0.75, (p) 0.8, (q) 0.9 vs Ag wire**

At the neutral state  $\lambda_{\max}$  value due to the  $\pi$ - $\pi^*$  transition of the copolymer was found to be 540 nm and  $E_g$  was calculated as 1.55 eV. Copolymer presents a weakened (and shifted)  $\pi$ - $\pi^*$  transition at 890 nm and yet a new transition around





1340 nm originates due to the charge carrier bands. Peaks around 890 and 1340 nm are attributed to the evolution of polaron and bipolaron bands respectively. Figure 3.18 represents the spectrum of copolymer in neutral state where a gradual shift and a broadening of the  $\lambda_{\text{max}}$  were observed with increasing potential. When the applied potential increased, intensity of  $\lambda_{\text{max}}$  peak decreased. Relatively high band gap for the copolymer results from the presence of BEBT where pristine PBEBT has a band gap of 1.6 eV. Table 3.4 is a good summary of comparison of the homopolymer, copolymer and PBEBT.  $\lambda_{\text{max}}$  value of the copolymer is between those of the PBEBT and the homopolymer. Thus,  $\lambda_{\text{max}}$  and  $E_g$  of the copolymer are considered to be in agreement with the expectations compared to parent polymers. These numerical values also support the copolymerization phenomenon. Copolymerization with BEBT provides multichromism and the color coordinates of the copolymer were determined by colorimetry in order to have an accurate objective measurement (Table 3.5).

**Table 3.4 Comparison of PTBPPQ, P(TBPPQ-co-BEBT) and PBEBT in terms of  $E_g$  and  $\lambda_{\text{max}}$  values**

	<b>PTBPPQ</b>	<b>P(TBPPQ-co-BEBT)</b>	<b>PBEBT</b>
$\lambda_{\text{max}}$	<b>408 nm</b>	<b>540 nm</b>	<b>618 nm</b>
<b><math>E_g</math></b>	<b>1.25 eV</b>	<b>1.55 eV</b>	<b>1.6 eV</b>



**Table 3.5 Electrochromic Properties of P(TBPPQ-co-BEBT)**

<b>Colors</b>	 <b>Purple</b>			 <b>Grey</b>			 <b>Light Green</b>			 <b>Transmissive Blue</b>		
	<b>Y</b>	<b>x</b>	<b>y</b>	<b>Y</b>	<b>X</b>	<b>Y</b>	<b>Y</b>	<b>X</b>	<b>y</b>	<b>Y</b>	<b>x</b>	<b>y</b>
<b>Copolymer</b>	<b>192</b>	<b>0.30</b>	<b>0.24</b>	<b>264</b>	<b>0.27</b>	<b>0.28</b>	<b>660</b>	<b>0.31</b>	<b>0.32</b>	<b>544</b>	<b>0.29</b>	<b>0.32</b>

### 3.2.3.3 Electrochromic switching of Poly(2,3-bis(4-tert-butylphenyl)-5,8-di(1H-pyrrol-2-yl) quinoxaline-co-4,7-bis(2,3-dihydrothieno[3,4-b][1,4]dioxin-5-yl)-2-dodecyl-2H-benzo [1,2,3] triazole) P(TBPPQ-co-BEBT)

To perform electrochromic switching studies, the polymer film was synthesized on ITO-coated glass slides in 0.1 M TBAPC in ACN. Switching properties of copolymer film were investigated by the application of potential square wave technique with a residence time of 5 seconds between - 0.5 V and +0.9 V.

Electrochromic contrast was reported as a percent transmittance change ( $\Delta T$  %) at 1320 nm where the electrochromic material has the highest optical contrast. The contrast was measured as the difference between  $T$  % in the reduced and oxidized forms and  $\Delta T$  % was noted as 59 % (Figure 3.19). Results showed that time required to reach 95 % of ultimate  $\Delta T$ % was less than 1 s which are again much faster than the typical switching times 1-2 s for an electrochromic polymer [101-105]. P(TBPPQ-co-BEBT) revealed highest optical contrast in the visible region which is 40 % (optical contrasts of homopolymer at 408 nm and 745 nm are 21 % and 12 % respectively and 23 % for copolymer with BiEDOT at 510 nm) in again less than 1 s. Hence, the copolymerization with BEBT was found to enhance also the optical contrast in the visible region with approximately the same switching time (switching time of P(TBPPQ-co-BiEDOT) was found to be 1.2 s at related wavelength). Table 3.6 is a good summary of comparison of the PTBPPQ, P(TBPPQ-co-BiEDOT) and P(TBPPQ-co-BEBT) in terms of transmittances and switching times. As it is clearly seen in the table P(TBPPQ-co-BEBT) shows highest transmittance in the visible region with a comparable transmittance in NIR.

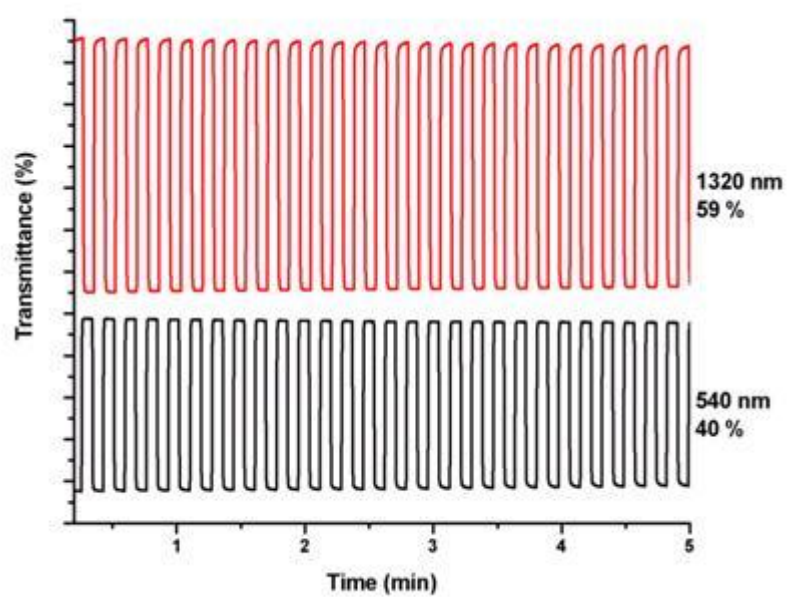


**Figure 3. 19 Electrochromic switching, optical absorbance change monitored at 540 nm and 1320 nm for P(TBPPQ-co-BEBT) in 0.1 M TBAPC/ACN**

**Table 3.6 Comparison of PTBPPQ, P(TBPPQ-co-BiEDOT) and P(TBPPQ-co-BEBT) in terms of transmittances and switching times**

	P(TBPPQ-co-BiEDOT)		P(TBPPQ-co-BEBT)		PTBPPQ	
$\lambda_{\max}$	510 nm	1320 nm	540 nm	1320 nm	408 nm	1480 nm
Optical contrast	23 %	57 %	42 %	59 %	21 %	65 %
Switching Time	1.2 sec	2.4 sec	$\leq 1$ sec	$\leq 1$ sec	$\leq 1$ sec	$\leq 1$ sec

## CHAPTER 4

### CONCLUSION

A novel pyrrole substituted quinoxaline derivative monomer was synthesized via Stille coupling reaction, and full characterizations of the materials were performed by NMR and Mass Analyses. The polymer of the corresponding monomer and its copolymers with BiEDOT and BEBT were synthesized by electrochemical methods. Cyclic voltammetry experiments, spectroelectrochemistry, kinetic studies and long-term switching experiments for the polymers were performed in order to enlighten the electrochemical and electrochromic properties.

Although many neutral state red and blue polymers were reported up to date, neutral state green polymeric materials appear to be limited. To obtain a green color there should be two distinct absorption bands one at red region and the other at blue region. Spectroelectrochemistry studies showed that homopolymer reveals two distinct absorption bands as expected for a donor-acceptor type green polymer, at 408 and 745 nm. This novel donor-acceptor type homopolymer was shown to be one of the few examples of neutral state green polymeric materials in literature. In addition, homopolymer has excellent switching times (0.1 sec, 0.3 sec, 0.6 sec) with outstanding optical contrast (65 %) in the NIR region.

Long-term stabilities even after 4000 cycles, ease of electrochemical synthesis and extremely fast switching times; make these polymers robust candidate for the completion of RGB color space.

As an easy method to combine desired properties, two copolymers of TBPPQ were achieved by electrochemical copolymerization. Resulting polymers have great potentials to be used in optoelectronic technology since they have multicolored states, fast switching times and high stabilities. Also studies showed that BEBT is a promising comonomer to improve optical and kinetic properties of electrochromic polymers.

Electrochromic investigations revealed that P(TBPPQ-co-BiEDOT) had lower band gap energy which showed the effect of BiEDOT on  $E_g$  with copolymerization. Moreover, copolymer showed mutlichromic property. Color tuning was achieved by changing the conjugation length along the backbone by copolymerization.

P(TBPPQ-co-BEBT) showed superior optical contrast in the visible region and faster switching time than P(TBPPQ-co-BiEDOT).

In conclusion, considering these advanced properties, many quinoxaline derivatives can be utilized in the polymer backbone for synthesis of new superior polymers to be used in electrochromic devices and electrochemical copolymerization can be considered to be a powerful tool to improve the electrochromic properties of quinoxalines, which were previously explored through the synthesis of its numerous derivatives.

## REFERENCES

- [1] M. Hatano, S. Kambara, S. Okamoto, J. Polym. Sci., 51 (1961) 26.
- [2] V. V. Walatka, M. M. Labes, and J. H. Perlstein, Phys. Rev. Lett., 31 (1973) 1139.
- [3] H. Lethebey, J. Chem. Soc, 15 (1862) 161.
- [4] H. Shirakawa, E. J. Louis, A. G. MacDiarmid, C. K. Chiang, A. J. Heeger, J. Chem. Soc., Chem. Commun., (1977) 578.
- [5] C. K. Chiang, C. R. Fischer, Y. W. Park, A. J. Heeger, H. Shirakawa, E. J. Louis, S. C. Gau, A. G. MacDiarmid, Phys. Rev. Lett., 39 (1977) 1098.
- [6] R. G. Mortimer, Chem. Soc. Rev., 26 (1997) 147.
- [7] J. H. Burroughes, D. D. C. Bradley, A. R. Brown, R. N. Marks, K. Mackay, R. H. Friend, P. L. Burns, A. B. Holmes, Nature (London, United Kingdom) 347 (1990) 539.
- [8] N. S. Sariciftci, L. Smiowitz, A. J. Heeger, F. Wudl, Science (Washington, DC, United States) 258 (1992) 1474.
- [9] J. Miasik, A. Hooper, B. C. Tofield, J. Chem. Soc. Farad. Trans. Phys. Chem. Cond. Pha., 82 (4) (1986) 1117.

- [10] H. Koezuka, A. Tsumura, *Synth. Met.*, 28 (1989) C753.
- [11] P. K. H. Ho, D. S. Thomas, R. H. Friend, N. Tessler, *Science*, 285 (1999) 233.
- [12] L. Bredas, G. B. Street, *Acc. Chem. Res.*, 18 (1985) 309.
- [13] M. Pomerantz, In *Handbook of Conducting Polymers*; 2nd ed.: b) T. A. Skotheim, R. L. Elsenbaumer, J. R. Reynolds, Ed: Marcel Dekker: New York, (1998) 227.
- [14] J. L. Dai, *Rev. Macromol. Chem. Phys.*, C39(2) (1999) 273.
- [15] J. I. Reddinger, J. R. Reynolds, *Adv. Polym. Sci.*, 45 (1999) 59.
- [16] K. Shimamura, F. E. Karasz, J. A. Hirsch, J. C. W. Chien, *Makromol Chem Rapid Commun*, 2 (1981) 473.
- [17] T. A. Skotheim, J. R. Reynolds, R. L. Elsenbaumer, *Handbook of conducting Polymers*, Marcel Dekker, New York, 1998 197.
- [18] X. Li, Y. Jiao, S. Li, *Eur. Polym. J.*, 27 (1991) 1345.
- [19] K. Pichler, D. A. Halliday, D. D. C. Bradley, P. L. Burn, R. H. Friend, A. B. Holmes, *J. Phys.: Condens. Matter*, 5 (1993) 7155.
- [20] M. G. Kanatzidis, *Chem. Eng. News*, 68 (1990) 36.



- [21] P. Chandrasekhar, *Conducting Polymers Fundamentals and Applications*, Boston, Kluwer Academic Publishers, (1999) Ch. 2.
- [22] A. G. MacDiarmid, A. J. Heeger, *Synth. Met.*, 1 (1979) 101.
- [23] A. D. Child, J. R. Reynolds, *J. Chem. Soc., Chem. Commun.*, 21 (1991) 1779.
- [24] A. G. MacDiarmid, *Synth. Met.*, 125 (2002) 87
- [25] K. E. Ziemelis, A. T. Hussain, D. D. C. Bradley, R. H. Friend, J. Rille, G. Wegner, *Phys. Rev. Lett.*, 66 (1991) 2231.
- [26] P. J. Nigrey, A. G. MacDiarmid, and A. J. Heeger, *Chem. Commun.*, 96 (1979) 594.
- [27] A. G. MacDiarmid, *Angew. Chem. Int. Ed.*, 40 (2001) 2581.
- [28] K. Gurunathan, A. V. Murugan, R. Marimuthu, U. P. Mulik, D. P. Amalnerkar, *Mater. Chem. Phys.*, 61 (1999) 173.
- [29] S. Alkan, L. Toppare, Y. Hepuszer, Y. Yağcı, *J. Polym. Sci. Part A: Polym. Chem.*, 37 (4218) 1999.
- [30] D. Kumar, R. C. Sharma, *Eur. Polym. J.*, 34 (1998) 1053.
- [31] T. Okada, T. Ogata, M. Ueda, *Macromolecules*, 29 (1996) 7645.
- [32] N. Toshima, S. Hara, *Prog. Polym. Sci.*, 20 (1995) 155.

- [33] K. Yoshino, R. Hayashi, R. Sugimoto, *Jpn. J. Appl. Phys.*, 23 (1984) 899.
- [34] Delabouglise, R. Garreau, M. Lemaire, J. Roncali, *New J. Chem.*, 12 (1988) 155.
- [35] A. Malinauskas, *Polymer*, 42 (2001) 3957.
- [36] R. H. Baughman, J. L. Bredas, R. R. Chance, R. L. Elsenbaumer, L. W. Shacklette, *Chem. Rev.*, 82 (1982) 209.
- [37] G. Zotti, *Handbook of Organic Conductive Molecules and Polymers*, ed. H. S. Nalwa, Wiley, Chichester, 1997, Vol. 2, Ch. 4.
- [38] J. Roncali, *Chem. Rev.*, 92 (1992) 711.
- [39] H. S. O. Chan, S. C. Ng, *Prog. Polym Sci.*, 23 (1998) 1167.
- [40] G. Tourillon, F. Garnier, M. Garzard, J. C. Dubois, *J. Electroanal. Chem.*, 148 (1983) 299.
- [41] S. H. Kim, J. S. Bae, S. H. Hwang, T. S. Gwon, M. K. Doh, *Pigments*, 33 (1997) 167.
- [42] A. Pennisi, F. Simone, G. Barletta, G. Di Marco, M. Lanza, *Electrochim. Acta*, 44 (1999) 3237.
- [43] N. Ozer, C. M. Lampert, *Thin Solid Films*, 349 (1999) 205.

- [44] C. O. Avellaneda, P. R. Bueno, R. C. Faria, L. O. S. Bulhoes, *Electrochim. Acta.*, 46 (2001) 1977.
- [45] Y. H. Huang, L. C. Chen, K. C. Ho, *Solid State Ionics*, 165 (2003) 269.
- [46] C. L. Lin, C. C. Lee, K. C. Ho, *J. Electroanal. Chem.*, 524 (2002) 81.
- [47] R. Jones, A. Krier, K. Davidson, *Thin Solid Films*, 298 (1997) 228.
- [48] G. Sonmez, *Chem. Commun.*, 42 (2005) 5251.
- [49] O. Tillement, *Solid State Ionics*, 68 (1994) 9.
- [50] A. Cirpan, L. Ding, F. Karasz, *Synth. Met.*, 150 (2005) 195.
- [51] J. Roncali, *Macromol. Rapid Commun.*, 28 (2007) 1761.
- [52] R. D. McCullough, *Adv. Mater.*, 10 (1998) 93.
- [53] F. Wudl, M. Kobayashi, A. J. Heeger, *J. Org. Chem.*, 49 (1984) 3382.
- [54] J. Roncali, *Chem. Rev.*, 97 (1997) 173.
- [55] C. J. Dubois, PhD Thesis, University of Florida, (2003).
- [56] T. Yamamoto, Z. H. Zhou, T. Kanbara, M. Shimura, K. Kizu, T. Maruyama, Y. Nakamura, T. Fukuda, B. L. Lee, N. Ooba, S. Tomaru, T. Kurihara, T. Kaino, K. Kubota, S. Sasaki, *J. Am. Chem. Soc.*, 118 (1996) 10389.

- [57] A. K. Agrawal, S. A. Jenekhe, H. Vanherzeele, J. S. Meth, J. Phys. Chem., 96 (1992) 2837.
- [58] G. Brocks, A. Tol, J. Phys. Chem., 100 (1996) 1838.
- [59] H. J. Ahonen, J. Lukkari, J. Kankare, Macromolecules, 33 (2000) 6787.
- [60] C. B. Gorman, R. C. West, T. U. Palovich, S. Serron, Macromolecules, 32 (1999) 41.
- [61] A. Battacharya, A. De, Prog. Solid. St. Chem., 24 (1996) 141.
- [62] R. Gumbs, Handbook of Organic Conductive Molecules and Polymers, ed. H. S. Nalwa, Wiley, Chichester, 1997, Vol. 2, Ch. 5
- [63] H. Koezuka, S. Etoh, J. Appl. Phys., 54 (1983) 2511.
- [64] K. K. Kanazawa, A. F. Diaz, W. Will, P. Grant, G. B. Street, G. P. Gardini, G. Kwak, Synth. Met., 1 (1980) 320.
- [65] S. Kuwabata, S. Ito, H. Yoneyama, J. Electrochem. Soc., 135 (1988) 1691.
- [66] O. Inganas, B. Liedberg, W. Hang-Ru, H. Wynberg, Synth. Met., 11 (1985) 239.
- [67] J. P. Ferraris, G. D. Skiles, Polymer, 28 (1987) 179.
- [68] H. S. Nalwa, Synth. Met., 35 (1990) 387.

- [69] S. R. Tseng, S. Y. Li, H. F. Meng, Y. H. Yu, C. M. Yang, H. H. Liao, S. F. Horng, C. S. Hsu, *Org. Electron.*, 9 (3) (2008) 279.
- [70] A. Balan, G. Gunbas, A. Durmus, L. Toppare, *Chem. Mater.*, 20 (24) (2008) 7510.
- [71] G. Sonmez, C. K. F. Shen, F. Rubin, F. Wudl, *Angew. Chem. Int. Ed.*, 43 (12) (2004) 1498.
- [72] A. Durmus, G. E. Gunbas, P. Camurlu, L. Toppare, *Chem. Commun.*, 31 (2007) 3246.
- [73] P. M. Beaujuge, S. Ellinger, R. Reynolds, *Adv. Mater.*, 20 (14) (2008) 2772.
- [74] S. A. Sapp, G. A. Sotzing and J. R. Reynolds, *Chem. Mater.*, 10 (1998) 2101.
- [75] B. C. Thompson, P. Schottland, K. Zong and J. R. Reynolds, *Chem. Mater.*, 12 (2000) 1563.
- [76] E. E. Havinga, W. Ten Hoeve, H. Wynberg, *Polym. Bull.*, 29 (1992) 119.
- [77] A. Berlin, G. Zotti, S. Zecchin, G. Schiavon, B. Vercelli, A. Zanelli *Chem.Mater.*, 16 (2004) 3667.
- [78] Nils-Krister, S. Mengtao, K. Par, P. Tonu, I. Olle, *J. Chem. Phys.*, 123 (2005) 204718.
- [79] U. Salzner, *J. Phys. Chem. B.*, 106 (2002) 9214.

- [80] H. A. M. van Mullekom, J. A. J. M. Vekemans, E. E. Havinga, and E. W. Meijer, *Mater. Sci. Eng., R.*, 32 (2001) 1.
- [81] A. B. Da Silveria Neto, A. Lopes Sant'Ana, G. Ebeling, S. R. Goncalves, E. V. U. Costa, H. F. Quina, J. Dupont, *Tetrahedron*, 61 (46) (2005) 10975.
- [82] Y. Tsubata, T. Suzuki, T. Miyashi, Y. Yamashita, *J. Org. Chem.*, 57 (25) (1992) 6749.
- [83] A. I. Vogel, in: B.S. Furniss, A. J. Hannaford, P. W. G. Smith, A. R. Tatchell (Eds.), *Vogel's Textbook of Practical Organic Chemistry*, fifth ed., Longman Scientific & Technical, England, 1989.
- [84] G. Y. Han, P. F. Han, J. Perkins, H. C. McBay, *J. Org. Chem.*, 46 (23) (1981) 4695.
- [85] C. Chen, Y. Wei, J. Lin, M. V. R. K. Moturu, W. Chao, Y. Tao, C. Chen, *J. Am. Chem. Soc.*, 128 (34) (2006) 10992.
- [86] H. Salman, Y. Abraham, S. Tal, S. Meltzman, M. Kapon, N. Tessler, S. Speiser, Y. Eichen, *Eur. J. Org. Chem.*, 11 (2005) 2207.
- [87] G. A. Sotzing, J. R. Reynolds, P. J. Steel, *Adv. Mater.*, 9 (1997) 795.
- [88] A. Kumar, D. M. Welsh, M. C. Morvant, F. Piroux, K. A. Abboud, J. R. Reynolds, *Chem. Mater.*, 10 (3) (1998) 896.
- [89] G. Sonmez, H. Meng, Q. Zhang, F. Wudl, *Adv. Func. Mater.* 13 (9) (2003) 726.

- [90] U. Salzner, M. E. Kose, J. Phys. Chem. B., 106 (36) (2002) 9221.
- [91] J. L. Bredas, R. R. Chance, R. Silbey, Phys. Rev., B 26 (10) (1982) 5843.
- [92] F. Ozyurt, E. G. Gunbas, A. Durmus, L. Toppare, Org. Electron., 9 (2008) 296.
- [93] Y. A. Udum, A. Durmus, G. E. Gunbas, L. Toppare, Org. Electron., 9 (2008) 501.
- [94] J. Tarabek, P. Rapta, E. Jaehne, D. Ferse, H. J. Adler, M. Maumy, L. Dunsch, Electrochim. Acta , 50 (7) (2005) 1643.
- [95] L. Dunsch, N. Andreas, P. Rapta, Fresenius J. Anal. Chem., 367 (4) (2000) 314.
- [96] A. Cirpan, A. A. Argun, C. R. G. Grenier, B. D. Reeves, J. R. Reynolds, J. Mater. Chem., 13 (10) (2003) 2422.
- [97] C. H. Yang, L. R. Huang, Y. K. Chih, S. L. Chung, J. Phys. Chem. 111 ( 2007) 3786.
- [98] S. Tarkuc, M. Ak, E. Onurhan, L. Toppare, J. Macr. Sci., Part A: Pure and Appl. Chem., 45 (2008) 164.
- [99] C. J. DuBois, K. A. Abboud, J. R. Reynolds, J Phys Chem., B 108 (2004) 8550.

[100] H. U. Yildiz, E. Sahin, I. M. Akhmedov, C. Tanyeli, L. Toppare, J Polym Sci Part A: Polym Chem., 44 (2006) 2215.

[101] C. L. Gaupp, J. R. Reynolds, Macromolecules, 36 (2003) 6305.

[102] P. Manisankar, C. Vedhi, G. Selyanathan, J Polym Sci Part A: Polym Chem., 45 (2007) 2787.

[103] D. M. DeLongchamp, M. Kastantin, P. T. Hammond, Chem Mater., 15 (2003) 1575.

[104] D. M. DeLongchamp, P. T. Hammond, Adv. Mater., 13 (2001) 1455.

[105] D. M. DeLongchamp, P. T. Hammond, Chem Mater., 16 (2004) 4799.